Oceanic Euxinia in Earth History: Causes and Consequences

Katja M. Meyer and Lee R. Kump

Department of Geosciences, The Pennsylvania State University, University Park, Pennsylvania 16802; email: kmeyer@geosc.psu.edu

Annu. Rev. Earth Planet. Sci. 2008. 36:251–88

First published online as a Review in Advance on January 9, 2008

The *Annual Review of Earth and Planetary Sciences* is online at earth.annualreviews.org

This article's doi:
10.1146/annurev.earth.36.031207.124256

0084-6597/08/0530-0251$20.00

Key Words

phosphorus cycle, sulfur cycle, ocean circulation, anoxia, geochemical proxies, mass extinction

Abstract

Euxinic ocean conditions accompanied significant events in Earth history, including several Phanerozoic biotic crises. By critically examining modern and ancient euxinic environments and the range of hypotheses for these sulfidic episodes, we elucidate the primary factors that influenced the generation of euxinia. We conclude that periods of global warmth promoted anoxia because of reduced solubility of oxygen, not because of ocean stagnation. Anoxia led to phosphate release from sediments, and continental configurations with expansive nutrient-trapping regions focused nutrient recycling and increased regional nutrient buildup. This great nutrient supply would have fueled high biological productivity and oxygen demand, enhancing oxygen depletion and sulfide buildup via sulfate reduction. As long as warm conditions prevailed, these positive feedbacks sustained euxinic conditions. In rare, extreme cases, euxinia led to biotic crises, a hypothesis best supported by evidence from the end-Permian mass extinction.

INTRODUCTION

OAE: oceanic anoxic event

Euxinia: a state of a body of water characterized by the presence of free hydrogen sulfide

Mass extinction: an event in Earth history during which more than 25% of all living families of organisms go extinct

Meromictic: a type of lake characterized by stable stratification: not subject to seasonal overturn

The deep ocean today is well oxygenated thanks to a conveyor-belt circulation that carries cold, oxygen-rich waters from high latitudes to the distant reaches of the abyssal zone. This condition is less robust that one may think; today, half of the oxygen injected into the deep sea in the North Atlantic deep-water formation regions is consumed during the decomposition of organic detritus settling through the water column. A doubling of the ocean's nutrient content could stimulate surface biological productivity and the export of detritus to the deep sea, leading to widespread anoxia.

During particular intervals of Earth history, the so-called oceanic anoxic events (OAEs), the deep ocean indeed became oxygen depleted. The causes and consequences of OAEs have been the subject of a number of thorough reviews (e.g., Arthur & Sageman 1994, Arthur & Sageman 2005, Strauss 2006). Under oxygen-free conditions, microbes reduce alternate electron acceptors during decomposition. After the small trace metal and nitrate reservoirs are depleted, sulfate reduction ensues. In many OAEs, then, anoxia evolved into euxinia, a state in which hydrogen sulfide concentrations built up to toxic levels in deep waters. The word euxinia is derived from the Greek name for the Black Sea, *Euxeinos Pontos*, or Hospitable Sea (King 2004), an irony that was not apparent to the early inhabitants whose exploration was restricted to oxygenated surface waters. Euxinia is rare today; however, euxinia was a defining characteristic of many key intervals of Earth history. Euxinic conditions may have prevailed during the Proterozoic, and have been associated with mass extinction in the marine realm and, curiously, the terrestrial realm at times in the Phanerozoic.

This review focuses on factors that influence the development of euxinia with an overall goal of developing a comprehensive model to explain euxinia that fits observations of both modern and ancient systems. We begin with a review of modern euxinic environments, identifying common characteristics essential for euxinia. Proxies used to identify euxinic environments in the geologic past are discussed and then applied to a survey of ancient euxinic environments. We then provide an analysis of the prominent hypotheses for the cause of euxinia. In doing so, we challenge the widespread opinion that ocean stagnation is an integral part of oceanic anoxia and euxinia. A conceptual model for widespread oceanic euxinia is proposed, which involves positive feedbacks that result once a favorable climate (warm) and continental configuration (abundant nutrient traps) have been established. We then explore the transition to a euxinic state, focusing on perturbations to the nitrogen cycle as oxygen is removed from seawater. Finally, we consider the role that euxinia may have played in mass extinctions during the Phanerozoic.

MODERN EUXINIC ENVIRONMENTS

The modern ocean is strongly stratified but largely oxygenated. In contrast to long intervals of Earth history, when euxinic conditions may have been ubiquitous (Canfield 1998), persistently euxinic waters today are rare. Seasonal euxinia develops in a wide variety of water bodies throughout the world, but the dominant settings for persistent euxinia are silled basins, meromictic lakes, coastal upwelling zones, and fjords. These

stratified water masses share physical and biogeochemical characteristics that include basin morphology, distinct sources of saline and fresh water, and elevated nutrient levels that support exceptional primary productivity. These modern euxinic environments provide field laboratories for developing and calibrating proxies that are used to interpret patterns in anoxic and euxinic paleoenvironments. In this section, we present examples of each type of euxinic basin and highlight commonalities between them.

GSB: green sulfur bacteria (anoxygenic phototrophs)

Silled Basins: The Black Sea

The Black Sea is the largest modern euxinic basin on Earth and covers roughly 4.4×10^5 km^2. Euxinia in the modern Black Sea results from a confluence of strong density stratification, weak ventilation of the chemocline, and elevated primary productivity that in turn induces high O_2 demand. Like the open ocean, the Black Sea experiences both wind-driven and thermohaline circulation (Murray et al. 2007). A thick suboxic layer separates oxic surface waters (0–50 m) from deep sulfidic waters (>100 m depth). Dense, nutrient-rich water enters only via the narrow Bosporus Strait to the south; large rivers provide fresh surface water via continental runoff from Eastern Europe. These two inputs generate strong density stratification in the Black Sea, with a deep-water residence time of ~300 years (Murray et al. 2007). Numerical modeling by Oguz (2002) demonstrates that stable density stratification allows ventilation of only the top 60 m of the water column. Their results suggest that even a dramatic cooling would not initiate oxygen injection into the sulfidic deep layer.

The expanded suboxic zone has both low oxygen and low sulfide concentrations (<10 μM). Abiotic and microbial processes cycle nitrogen and trace metals across the chemocline. Notable among the chemocline microbial population are the photosynthetic green sulfur bacteria (GSB, *Chlorobiaceae*). These anoxygenic sulfide-oxidizers can use irradiance that is just 0.0005% of the light available in surface waters (Overmann et al. 1992). Derivatives of the GSB light-harvesting carotenoid, isorenieratene, are preserved in anoxic sapropels of the Black Sea. The distribution of this molecular fossil in sediment cores from near the modern chemocline is thought to record chemocline depth oscillations over the past 8 kyr (Huang et al. 2000).

Fjords: Framvaren and Mariager

Fjords are glacially carved, long, narrow marine inlets with steep walls. Often, a constriction between the fjord and open ocean limits water exchange and restricts the supply of dense, oxic water to the fjord bottom. Here, we focus on two fjords in the North Sea, the Framvaren and Mariager fjords.

Framvaren Fjord in southern Norway is a long, deep euxinic basin that supports the highest hydrogen sulfide concentrations of any modern saline system (Anderson et al. 1988, Millero 1991). Isostatic rebound following deglaciation isolated the fjord and it became a meromictic lake. In 1850, a shallow (~2.5 m depth) channel was dug to connect the lake to neighboring Hellvikfjord, transforming the lake into a fjord (Skei 1988). A chemocline at 18–20 m separates sulfidic, saline Framvaren bottom water

FGL: Fayetteville Green Lake (New York, USA)

PSB: purple sulfur bacteria (anoxygenic phototrophs)

(7–8 mM sulfide) from less dense surface waters. Since 1850, two recorded seawater incursions through the channel, in 1902 and 1942, caused chemocline shallowing and fish kills. The second event in 1942 was sufficient to cause the chemocline to raise to the air-water interface, causing widespread fish mortality in the fjord (Skei 1988).

Mariager Fjord is located in the Jutland region of Denmark. It is 30 km long and ~2 km wide, with a long, shallow channel connecting it to the sea. A permanent halocline is located at 10–15 m depth, whereas the chemocline fluctuates from 10–25 m; this variation depends on temperature through effects on metabolic rates, and the delivery of O_2 from wind mixing (Fallesen et al. 2000). A three-year study of the sulfur cycle by Sorensen & Canfield (2004) found most sulfide is produced in the sediments and invades the deep layer through diffusion. Deep-water sulfide concentrations range from 100–1100 uM.

The Mariager chemocline is highly dynamic, and local observations of the smell of H_2S in the air surrounding the fjord suggest the chemocline rose to the air-sea interface during the summers of 1933, 1947, 1970, and 1997. In 1997, the evasion of sulfide from the surface layer decimated eukaryotes living above 8 m water depth. It washed dead fish, grasses, and benthic species such as mussels to shore and produced a sudden pulse of free sulfur that turned the water a milky color. Phosphate released from sediments quadrupled the PO_4 content of the surface water (12.6 μM phosphate). Ammonium concentrations more than doubled owing to widespread decomposition, and the excess nutrients caused a diatom bloom (Fallesen et al. 2000). The primary influences responsible for this event were warm air temperatures, decreased wind-mixing, eutrophication, and biological feedbacks (Fallesen et al. 2000).

Meromictic Lakes

Although the majority of freshwater lakes turn over at least once each year, meromictic lakes remain stably stratified (unmixed). Investigators intensively study meromictic lakes because of their distinctive microbial chemocline communities, rare geochemistry, and laminated sedimentary records.

Fayetteville Green Lake (FGL), New York, was the first meromictic lake identified in the United States (Eggleton 1931). Formed as a glacial plunge pool during the last deglaciation (Thompson et al. 1990), the lake is deep (55 m) but small (460 m diameter). Dense, sulfate-rich groundwater discharges from a surrounding deep aquifer directly to the dense monimolimnion. A sharp chemocline at ~21.5 m separates the slightly denser sulfidic deep water from oxic less-dense surface water (Brunskill & Ludlam 1969). Maxima in primary productivity occur at 9 m depth and in the chemocline, where a dense community of purple and green sulfur bacteria thrive (Thompson et al. 1990).

Like FGL, the alpine Lake Cadagno (Switzerland) formed as glaciers receded, and has sulfate-rich deep water owing to the influence of gypsum in the surrounding watershed (Del Don et al. 2001). The chemocline at 9–14 m depth also supports a community of purple sulfur bacteria (PSB). Small, uncultured purple sulfur bacteria dominate the chemocline, although PSBs *Ameobobacter purpureus*, *Lamprocystis*

reseopersicina, and *Chromatium okenii* are also abundant. *Chlorobium phaeobacteroides* is the most abundant green sulfur bacterium. During months when light intensities are relatively low, the chemocline community does not exhibit a vertical structure, but population stratification of the chemocline occurs during times of high light intensity (Tonolla et al. 2003).

In western Canada, an alkali composition of surrounding lavas in the watershed influences meromictic Lake Mahoney. Lake Mahoney is salinity stratified owing to the separate sources of fresh surface water and relatively dense deep water that have percolated through the lavas. The chemocline at 6 m depth hosts a dense PSB population dominated by *Ameobobacter purpureus* (Overmann et al. 1991). Preservation of the PSB carotenoid okenone in Mahoney sediments records an 11,000-year history of meromixis (Overmann et al. 1993).

Unifying Characteristics of Modern Euxinic Environments

The euxinic basins discussed here share many physical and biogeochemical characteristics (see **Table 1**). Many of them exhibit restricted circulation, are deep relative to their surface area, and support high primary productivity because of elevated nutrient concentrations. Although conventional wisdom holds that sluggish circulation is the primary reason for euxinia, the argument can be made that nutrient trapping is the fundamental characteristic that promotes euxinia in these basins. If so, then the restricted circulation characteristic of many modern euxinic basins is important because it promotes nutrient trapping, not because it slows circulation rates.

Modern euxinic environments display a strong positive relationship between deep water [PO_4] and sulfide concentration (**Table 1**, **Figure 1**; Shen et al. 2002). This correlation is understandable from biogeochemical relationships: As decomposition proceeds in deep waters, oxidant is consumed and stoichiometric amounts of waste product (including H_2S and organic-bound N and P) are released. Thus, the expectation is that phosphate and H_2S should covary. According to the stoichiometry of

Table 1 Characteristics of modern euxinic basins

	Black Sea	Framvaren Fjord	Mariager Fjord	Fayetteville Green Lake	Lake Cadagno	Lake Mahoney	Cariaco Basin
Surface area (km^2)	420325	4.43	–	0.258	0.261043	0.198	–
Volume (km^3)	541220	0.33	–	7.236	2.41985	–	–
Surface/volume (km^{-1})	0.77	13.4	–	0.04	0.11	–	–
Chemocline depth (m)	120–180	18	8–18.00	21.5	8–10 m	6.5–7 m	200 m
PO_4 (μM) surface	–	–	3	0.41	–	–	–
PO_4 (μM) deep	7.7	100	20	3	–	–	3.7
N/P deep	12	15	30	>100	–	–	–
H_2S (μM) deep	310–3600	7000–8000	<400–1100	1200	175–235	3000–4000	76
$\delta^{13}C$ gradient	6‰	17‰	–	13.1‰	–	–	–

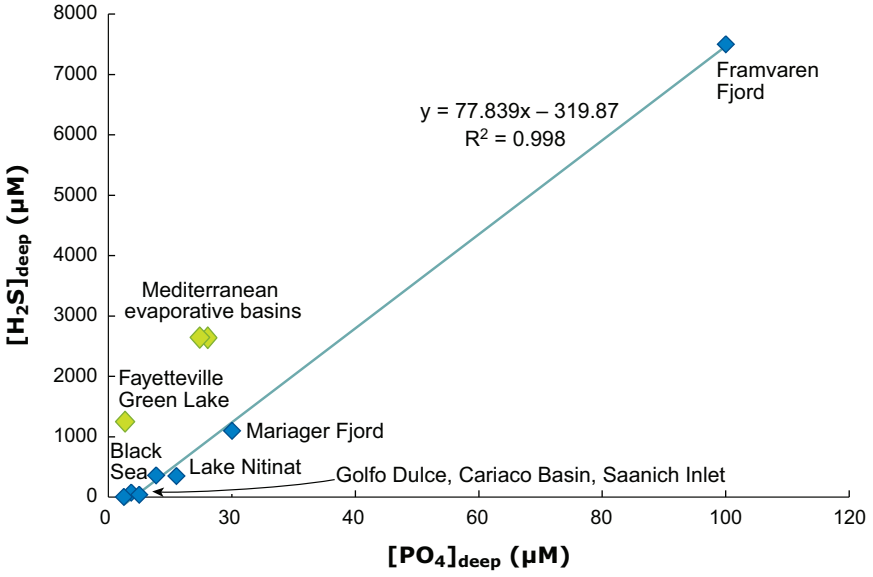

Figure 1

Relationship between phosphate and hydrogen sulfide concentrations in the deep waters of modern euxinic basins (data from **Table 1**). Mediterranean hypersaline basins and Fayetteville Green Lake (FGL) have higher sulfide concentrations than expected based on phosphate concentrations. The Mediterranean basins may have lost phosphate owing to mineral precipitation during evaporation (Shen et al. 2002); FGL has excess sulfide input from groundwater sources.

microbial sulfate reduction,

$$2CH_2O + SO_4^{2-} \rightarrow 2HCO_3^- + H_2S,$$

approximately 2 moles of organic C are oxidized per mole of sulfate reduced. The amount of phosphate released is determined by the Redfield ratio (C/P) of the organic matter being remineralized. The C/P of organic material implied by the slope in **Figure 1** is $2 \times 78 = 156$, which is within the range of values for particulate organic matter in the euphotic zone of the Black Sea [126–231 (Yilmaz et al. 1998)] and in sediment traps from normal marine systems (e.g., Broecker & Peng 1982), but higher than the canonical Redfield value of 106 because of preferential recycling of P and P-deficient biological uptake. The *x*-intercept, interpreted as the approximate threshold for euxinia, is at $[PO_4] = 4.1$ μM. With a Redfield ratio of O_2:P of 106, this represents an oxygen demand of approximately 435 μM, sufficient to deplete the coldest bottom waters of oxygen (~350 μM) and nitrate. As phosphate concentrations rise above this threshold, hydrogen sulfide begins to accumulate in the basin.

Diagenesis: chemical and physical transformations of sediment and entrapped pore waters from the time of deposition until higher temperatures and pressures lead to metamorphism

In their numerical analysis of the causes of euxinia in silled basins, Shen et al. (2002) found that anoxia is favored when riverine input of nutrients is high, when recycling of P during diagenesis is high (P burial efficiency low), and when the rate of

vertical mixing within the basin is suppressed relative to the deep inflow rate. To the extent that the deep inflow into a silled basin is equivalent conceptually to the global thermohaline circulation rate, this result is entirely consistent with our conclusion that ocean stagnation is not conducive to the development of oceanic euxinia.

Rather, silled basins with estuarine circulation, such as the Black Sea and some fjords, are efficient nutrient traps. Estuarine flow occurs in stratified water bodies that experience a positive water balance (where riverine input and/or precipitation rates exceed evaporative losses) (Demaison & Moore 1980). Low salinity, nutrient-depleted surface water flows out of the basin, while salty, nutrient-replete waters enter the basin at depth. These nutrient-rich deep waters are mixed upward, promoting biological productivity, which in turn creates a high oxygen demand as the organic matter falls through the water column. Riverine input provides an important additional source of nutrients to modern euxinic basins. Biological pumping within the basin maintains the nutrient gradient between surface and deep waters and enhances nutrient trapping by maintaining nutrient-poor surface waters.

In modern euxinic systems without estuarine circulation, other factors aid in sulfide accumulation. For example, the groundwater supply to many meromictic lakes is sulfur (often sulfate and sulfide) replete. This additional sulfide source allows H_2S accumulation independent of phosphate concentration. Finally, in shallow eutrophied environments like Mariager Fjord, sulfate reduction in the organic-matter-laden sediments produces the bulk of sulfide, which diffuses upward into the water column. This mechanism is unlikely to account for persistent euxinia in open marine environments, although sulfide flux from sediments is observed periodically in the modern Benguela upwelling zone [off the coast of Namibia (Weeks et al. 2004)].

Black shale: a dark-colored, fine-grained sedimentary rock; the dark coloration occurs because of relatively high concentrations of preserved organic matter

PROXIES FOR EUXINIA

Our analysis of modern euxinic basins has identified some shared factors that contribute to the euxinic state. We can use this knowledge to help interpret the conditions that led to oceanic euxinia in the past, but it is not necessarily obvious how one identifies euxinic basins in the rock record. Several proxies for euxinia have been proposed; we describe and evaluate these below.

S/C Ratios in Sediments

Historically, interest in identifying intervals of oceanic euxinia arose from a desire to better understand the formation mechanisms of sedimentary pyrite and their relationship to conditions that promote the accumulation of organic matter. Some sedimentary rocks, in particular marine black shales, are extraordinarily enriched in pyrite. These enrichments are often interpreted to be primary or early diagenetic features (Raiswell & Berner 1985). Typical marine shales deposited from oxic waters have S contents (mostly as pyrite, FeS_2) that track organic carbon (C_{org}) content (Berner & Raiswell 1983). This association between pyrite and C_{org} indicates that those processes that lead to the preservation of organic carbon tend to promote the preservation of pyrite. Berner & Raiswell (1984) interpret sediments depleted in S

DOP: degree of pyritization (fraction of reactive Fe that is present as pyrite)

relative to C_{org} as nonmarine, and those enriched in S relative to C_{org} as deposited under euxinic waters where pyrite precipitation in the water column may have decoupled S contents from C_{org} preservation (Raiswell & Berner 1985). On plots of S versus C_{org} content, euxinic sediments are expected to show S contents that are relatively invariant with changes in C_{org}, with a positive S intercept reflecting the portion of pyrite formed in the water column. In contrast to this expectation, deep basinal Black Sea sediments display S depletions relative to C_{org}. This unexpected relationship may result from Fe availability limiting pyrite formation (Calvert & Karlin 1991, Lyons & Berner 1992), but it does complicate the use of S/C ratios to infer euxinia.

Degree of Pyritization

Under euxinic conditions the supply of reactive iron (i.e., phases of Fe that will react with free sulfide to form pyrite) can limit the amount of pyrite formed. If so, then Fe in euxinic sediments should show a large degree of pyritization (DOP) (Raiswell et al. 1988) defined as the ratio of pyrite Fe to total reactive Fe (digestible in HCl, an imperfect proxy for reactivity during early diagenesis). Raiswell et al. (1988) show that DOP is a better discriminant of sediments deposited under oxic, anoxic, and euxinic bottom-water conditions than S/C ratios. However, particular environments, e.g., salt marshes, display DOP values that span the range from well oxygenated to highly euxinic (Roychoudhury et al. 2003). Moreover, it is likely that the high DOP values of deep Black Sea sediments have been enhanced by reactive Fe mobilization through diagenesis on the shelf and transport into the basin. Thus, DOP should be high in euxinic environments, but caution should be exercised in basing such conclusions on DOP alone.

Highly Reactive Fe Content

The remobilization of Fe in shelf settings and transfer to the deep leads to an increase in the ratio of highly reactive to total Fe [Fe_{HR}/Fe_T (Raiswell & Canfield 1998)] and of total Fe to Al (Fe_T/Al_T) in basinal sediments (Lyons & Severmann 2006). Fe_{HR} includes FeS, FeS_2, and any iron that can be extracted in a buffered citrate-dithionite leach. It does not include the poorly reactive Fe that can be leached from recalcitrant phases under the boiling acid treatment, the approach earlier used to define reactive iron for DOP (Raiswell & Canfield 1996). Of course, other mechanisms can enhance highly reactive iron contents of sediments, including hydrothermal input of Fe or focusing of iron-oxide deposition in the generation of banded iron formations. Thus, elevated Fe_{HR}/Fe_T may be considered a characteristic but not diagnostic indicator of euxinia.

Pyrite Size Distribution

Pyrite formation in the water column of euxinic basins is a phenomenon reflected in the size distribution of pyrite grains, given the contrasting times available for formation in the water column compared with the sediments. This size discrimination

was observed in a study of various euxinic and noneuxinic basins by Wilkin et al. (1996). Pyrite grains in sediments beneath euxinic deep water had a narrower size distribution and were on average smaller than those formed in sediments under an oxic water column. This proxy has been applied with success to Late Permian sediments by Nielsen & Shen (2004) and Wignall & Newton (2003). To the extent that size distributions are not affected by diagenetic ripening and overgrowths, this proxy seems to be a robust indicator of euxinic conditions.

Sulfur Isotopic Composition

The process of sulfate reduction is associated with a significant isotopic discrimination, with the product sulfide being depleted in the heavier isotope by approximately 30‰ as long as sulfate is plentiful (Habicht et al. 2002). In a closed system, as sulfate becomes depleted, the isotopic difference between sulfide and sulfate diminishes. Pyrite formed in euxinic water columns thus should be isotopically light relative to diagenetic pyrite formed in sediments, which more closely represent closed systems. The $\delta^{34}S$ of pyrite in Unit 1 of the Black Sea is isotopically light, with values of ~–35 per mil, reflective of the ^{34}S-depleted isotopic composition of aqueous sulfide (Calvert et al. 1996). Pyrite from earlier phases of Black Sea sedimentation displays positive values of $\delta^{34}S$ reflective of increased sulfate limitation. Typical modern marine pyrite displays a range of values indicative of the degree of sulfate depletion during early diagenesis (Canfield et al. 1992). Thus, the use of $\delta^{34}S$ as a euxinic proxy is complicated by environmental Rayleigh distillation. As we describe below, euxinic basins identified in the rock record tend to be isotopically heavy, reflecting intense sulfate reduction in basins with initially low sulfate concentrations. To our knowledge, there is a dearth of arguments in the literature for euxinia based on observations of isotopically light sulfur.

Trace-Element Enrichment

Like iron, redox conditions control the mobility of many other trace elements in sediments. Relative enrichment or depletion of these redox-sensitive trace elements serves as a redox indicator of the overlying water. For example, Algeo & Maynard (2004) describe strong enrichments in Mo, U, V, and Zn from sediments deposited under euxinic bottom waters; Brumsack (2006) extends this list to include Cd, Cu, Tl, Ni, and Sb. These metals all have in common the tendency to form insoluble phases under anoxic and sulfidic conditions.

Consideration of widespread, globally significant euxinia forces us to reconsider the modern analog approach for trace-metal enrichment. For example, modern euxinic basins have sediments enriched in Mo. However, persistent euxinia would be expected to gradually lower the Mo concentration of seawater as expanded sinks exceeded riverine sources. This Mo decrease is observed in the Late Devonian shales of the central Appalachian Basin: Mo contents of black shales decline with time as other indicators of euxinia (e.g., DOP) increase (Algeo 2004). Subsequent study of modern euxinic basins has confirmed the generalization that with time, euxinic basins become

depleted in Mo. Although Mo is a less-than-straightforward indicator of basinal euxinia (Algeo & Lyons 2006), its isotopic composition may reflect the areal extent of anoxic and/or sulfidic deep waters if the Mo reservoir is sufficiently large and well mixed (Arnold et al. 2004).

C/P Ratio

In modern anoxic sediments, phosphorus is preferentially regenerated relative to organic carbon (Ingall et al. 1993). As a result, sediments beneath anoxic water columns exhibit higher C/P ratios in preserved organic matter (Ingall & Jahnke 1997). Explanations for this phenomenon include desorption of phosphate from iron-oxide particles as they become reduced under anoxic/reducing conditions, and less retention of phosphate by anaerobic bacteria (Ingall et al. 1993). However, the extent of this organic matter P-enrichment in modern anoxic settings is quite variable. For example, downcore trends at Saanich Inlet are subdued relative to other locations and in comparison to many other black shales (Filippelli 2001). In support of this proxy, bioturbated sediments from the Devonian-Mississippian New Albany shales consistently have smaller C_{org}/P_{org} values (~150) than laminated shales (~3900) (Ingall et al. 1993). Several other ancient shales display elevated C/P ratios consistent with anoxic (and perhaps euxinic) depositional settings.

Organic Biomarkers

Biomarkers from members of microbially dominated photosynthetic chemocline communities serve as a promisingly robust proxy for photic zone euxinia in ancient sediments. The characteristic GSB and PSB require both light and sulfide and contain unique photosynthetic pigments that can be recorded in sediments. For example, the *Chlorobiaceae* (GSB) contain the carotenoid isorenieratene. The burial products of isorenieratene, including isorenieratane, tetramethylbenzenes, and aryl isoprenoids, formed during diagenesis or catagenesis have been isolated from sedimentary rocks as old as ~1.6 Ga (Hartgers et al. 1994, Koopmans et al. 1996a, Damste et al. 2001, Brocks et al. 2005). GSB use the reverse TCA cycle to fix carbon. As a result, molecular fossils of GSB tend to have relatively large $\delta^{13}C$. This isotopic signature distinguishes GSB-derived molecules from similar isoprenoid products of beta-carotene decomposition that are synthesized via Calvin cycle–dependent organisms (Koopmans et al. 1996b). Bacteriochlorophyll-derived maleimides are another useful marker of GSB (Grice et al. 1996). Additionally, diagenetic products of the carotenoids chlorobactene and okenone record the presence of *Chlorobiaceae* (GSB) and *Chromatiaceae* (PSB), respectively (Brocks et al. 2005). One final compound, gammacerane, is an indirect marker of euxinia. This compound is derived from tetrahymanol, which is synthesized by ciliates with a sterol-poor diet. Because sterols are ubiquitous in eukaryotes, the presence of gammacerane implies that the ciliates were grazing on prokaryotes, and stable isotopic evidence indicates that the diet is green sulfur bacteria (Damste et al. 1995). Gammacerane has been identified in diverse ancient environments, including stratified marine, lacustrine, and hypersaline settings.

The presence of these biomarkers in basinal marine sediments is quite likely the definitive proxy for euxinia, with a caveat: They could potentially represent materials that were transported from shallow-water sites where microbial mats were abundant. Careful facies analysis must be performed to rule out this possibility. Of course, all biomarker interpretations are subject to revision based on discoveries of new pathways to their formation, but the presence of the suite of biomarkers listed above is likely to remain a definitive indication of water-column euxinia.

BIF: banded iron formation

ANCIENT EUXINIC BASINS

Combinations of the proxy indicators described above have been applied to the analysis of sedimentary rocks to identify ancient basins with euxinic water columns (**Table 2**). Here we progress through Earth history describing the occurrences of euxinia and relating them to the environmental conditions, both local and global, that sustained them. We begin with the Proterozoic because Archean shales lack the high S/C ratios and other proxy indicators of euxinia (Raiswell & Berner 1985, Watanabe et al. 1997). Apparently, the Archean ocean had low marine sulfate concentrations, likely because of the absence of oxidative weathering on land that in subsequent times provided a large source of riverine sulfate to the ocean (Habicht et al. 2002).

The Proterozoic

Strong evidence now exists that atmospheric oxygen levels rose dramatically and permanently at around 2.45 Ga, heralding the transition to an aerobic biosphere (Melezhik et al. 2005 and references therein). In a counter-intuitive way, the "rise of oxygen" allowed for the development not only of highly oxidizing but also strongly reducing environments such as euxinic marine basins. Recognition of this has led to interesting alternative hypotheses for the cause of the demise of the signature Precambrian banded iron formations at the beginning, and the explosion of metazoan life at the end of the Proterozoic.

Euxinia and the end of banded iron formation deposition. Banded iron formations (BIFs) are well represented in the Archean and Paleoproterozoic rock record, but disappear at ~1.8 Ga. The conventional wisdom has held that the deep ocean became mildly oxidizing after 1.8 Ga, preventing the accumulation of aqueous Fe (Holland 2006). This premise has been challenged by Canfield (1998), who proposed that instead of oxygenation, the deep ocean became sulfidic at approximately 1.8 Ga as a natural consequence of the buildup of the seawater sulfate reservoir. According to Canfield, the Paleoproterozoic and Mesoproterozoic atmospheres contained sufficient oxygen to stimulate oxidative weathering of sulfides on land, but insufficient oxygen to keep the deep ocean oxygenated. Sulfide weathering led to a marked increase in riverine sulfate flux to the ocean. Ocean sulfate concentrations increased, supported by evidence of an increasing spread in $\delta^{34}S$ of the sedimentary pyrite record from 2.7 Ga to 2.2 Ga (Canfield 1998). This time also coincides with the first appearance of sulfate mineral evaporites in the geologic record (Melezhik et al. 2005).

Table 2 Characteristics of ancient euxinic basins

Name	Age	Proxy indicators										Basin characteristics	References
		S/C	DOP	Fe_{HR}/Fe_T	Fe_T/Al_T	Pyrite size	$\delta^{34}S$	Trace metal	Mo isotope	C/P	Biomarker		
Rove	1.8 Ga	x		x			x					Open continental shelf	Poulton et al. 2004
Vindhyan	1.7 Ga	x										Epicontinental sea	Banerjee et al. 2006
Woologorang	1.7 Ga	x	x	x			x		x			Intracratonic with opening to sea	Shen et al. 2002, Arnold et al. 2004
Barney Creek	1.64 Ga										x	Deep marine rift basin	Brocks et al. 2005
Reward	1.6 Ga	x	x	x			x					Intracratonic with opening to sea	Brocks et al. 2005
Roper Group	1.5 Ga		x	x			x		x			Intracratonic with opening to sea	Shen et al. 2003, Arnold et al. 2004
Nonesuch	1.0 Ga	x										Lacustrine intracontinental rift	Imbus et al. 1992
Vazante Group	Sturtian										x	Marine, below storm wave base	Olcott et al. 2005
Selwyn	Early Paleozoic						x					Restricted epicont. Marine basin	Goodfellow & Jonasson 1984
Ill/Mich Basins	Devonian/ Early Mississippian										x	Intracratonic basins	Brown & Kenig 2004

Oatka Crk (Appal. Basin)	Devonian		x		x			x				Foreland basin	Werne et al. 2002
New Albany (Appal. Basin)	Devonian/ Early Mississippian	x					x	x				Foreland basin	Ripley et al. 1990
Holy Cross	Devonian					x						Open shelf	Bond et al. 2004
Kellwasser (Appal. Basin)	Devonian									x		Foreland basin	Murphy et al. 2000
Cleaveland (Appal. Basin)	Devonian							x				Foreland basin	Algeo et al. 2004
Sunbury (Kentucky)	Mississippian	x	x					x				Foreland basin	Rimmer 2004
Kansas	Pennsylvanian	x	x					x				Semirestricted intracratonic seaway	Algeo & Maynard 2004
East Greenland	Late Permian					x	x				x	Intracratonic basin	Nielsen & Shen 2004, Hays et al. 2006
Kashmir	Late Permian					x						Deep-water continental margin	Wignall et al. 2005
South China	Late Permian						x				x	Carbonate platform to shelf	Grice et al. 2005, Newton et al. 2004, Riccardi et al. 2006

(*Continued*)

Table 2 (*Continued*)

Name	Age	Proxy indicators										Basin characteristics	References
		S/C	DOP	Fe_{HR}/Fe_T	Fe_T/Al_T	Pyrite size	$\delta^{34}S$	Trace metal	Mo isotope	C/P	Biomarker		
Ursula Creek BC	Late Permian					x		x				Deep continental margin	Wignall & Newton 2003
Perth Basin (Australia)	Late Permian						x				x	Above storm wave base	Grice et al. 2005 and references therein
Umbria	Toarcian										x	Continental margin	Pancost et al. 2004
Posidon (Germany)	Toarcian										x	Epicontinental sea	Schouten et al. 2000
Livello Selli	Aptian										x	Deep continental margin	Pancost et al. 2004
Shatsky Rise	Aptian	x										Open ocean >1 km depth	Dumitrescu & Brassell 2006
Demerara Rise	Cenomanian-Turonian							x				~2 km depth	Brumsack 2006
North Atlantic	Cenomanian-Turonian										x	Continental margin	Pancost et al. 2004
Tarfaya Basin (Morocco)	Cenomanian-Turonian									x		Pelagic sedimentation	Nederbragt et al. 2004

Sulfate subsequently became the most abundant oxidant in the deep sea, and the ocean turned euxinic. According to Canfield (1998), the Fe-rich to H_2S-rich ocean conversion may have taken several million years while the rate of Fe delivery exceeded production of H_2S until ~1.8 Ga, when BIF deposition ended.

Poulton et al. (2004) appear to have captured this transition to global euxinia in sediments spanning the end of BIF deposition (Gunflint Formation, Superior Province, Ontario, Canada) through a period of pyrite and organic-carbon-rich shale deposition (Rove Formation). This interpretation was supported by the multiple sulfur isotope study of Johnston et al. (2006), who also found evidence for H_2S release to the atmosphere from a chemocline that may have migrated to the sea surface.

The "Canfield Ocean" interval. Euxinia during the ensuing billion years is indicated by various proxies in a number of Proterozoic basins. High S/C ratios in black shales of the Vindhyan Supergroup of central India [~1.7 Ga (Banerjee et al. 2006)] indicate that this epeiric sea was euxinic. Phanerozoic-based S/C criteria must be applied with caution to Precambrian sediments because of possibly confounding effects of more reactive organic matter, subsequent diagenetic and metamorphic effects (Jackson & Raiswell 1991, Lyons et al. 2000), and potentially low seawater sulfate concentrations. Moreover, many of the Proterozoic basins, including the Midcontinental Rift (Imbus et al. 1992) and Mesoproterozoic Belt Supergroup of Montana, United States, have been variously interpreted as isolated lacustrine or restricted marine (Lyons et al. 2000).

The MacArthur Basin of northern Australia, in contrast, was demonstrably marine based on lithofacies analysis, and it represents a typical intracratonic setting open to the ocean with tidal influence (Jackson & Raiswell 1991, Shen et al. 2003). The older Wollogorang (1.7 Ga) and Reward (1.6 Ga) formations display high S/C and DOP values suggestive of euxinic conditions (Shen et al. 2002). Moreover, biomarkers for PSB and GSB have been identified from the underlying Barney Creek Formation (Brocks et al. 2005). Pyrite sulfur isotopic compositions approaching that of contemporaneous seawater, especially in the Reward Formation, support an interpretation of a sulfate-depleted water column (Shen et al. 2002). Subsequently, Shen et al. (2003) identify a sulfate minimum zone, comparable to the modern ocean oxygen-minimum zone, in the slightly younger Roper Group (1.5 Ga). Large fluctuations in sulfate content of Proterozoic carbonates are consistent with low seawater sulfate concentrations during this time (Kah et al. 2004, Gellatly & Lyons 2005).

What is the evidence, though, that the euxinic "Canfield Ocean" was indeed global in scope at any particular time in the Proterozoic? This question was recently addressed in McArthur basin sediments using Mo isotopic techniques (Arnold et al. 2004). If Mo isotopes were well mixed in the Proterozoic ocean, the values measured in Roper Group and Woologorang Group sediments are likely globally representative. Low ratios of $^{97}Mo/^{95}Mo$ are interpreted by Arnold et al. (2004) to reflect an expanded area of seafloor overlain by suboxic bottom waters and perhaps large regions of deep-water euxinia.

The end of Proterozoic euxinia. In its original conception (Canfield 1998), the Canfield Ocean ended in the Neoproterozoic with the resumption of banded iron formation contemporaneous with a putative rise in atmospheric oxygen. Canfield based this argument on an observed isotopic trend toward increasingly negative $\delta^{34}S$ values of pyrite linked to the increased importance of sulfur disproportionation by chemoautotrophic sulfur bacteria (Canfield & Teske 1996). However, more recent work shows that this metabolism was active by 1.3 Ga (Johnston et al. 2005). Moreover, there is limited evidence that euxinic basins existed during Snowball Earth, at least in some places. The Sturtian-aged (~740–700 Ma) Vazante Group of Brazil preserves dropstone-laden, glendonite-bearing, organic-carbon-rich shales with diverse biomarker assemblages. Biomarkers include 2,3,6-trimethylbenzene, which may have been derived from GSB, and gammacerane, supporting the interpretation that photic-zone euxinia existed contemporaneously with continental glacial conditions (Olcott et al. 2005), at least in one basin in Brazil. Most recently, Canfield et al. (2007) and Fike et al. (2006) argued that the oxygenation of the deep ocean occurred after the Gaskiers glaciation, approximately 580 Ma.

Summary. In summary, there is compelling evidence for episodes of widespread oceanic euxinia in the Proterozoic. In our opinion, however, the evidence for a persistently euxinic global Proterozoic ocean is not strong. In fact, compilations of black shale abundance, whether considered as cumulative thickness or as a proportion of total shale abundance, show peaks from 2.0–1.8 Ga and from 0.8–0.6 Ga (Condie et al. 2001). These peaks bracket the period of the proposed euxinic ocean, which is instead a time of low black shale abundance. This is rather curious, given the general observation that euxinic basins preserve high concentrations of organic matter. Chemical index of alteration data also are confusing in the context of the Canfield Ocean because they correlate with the black shale proportions. This suggests that the warm, moist intervals of the Proterozoic were before and after, but not during the Canfield Ocean interval. The black shales used to support the notion of persistent Proterozoic euxinia occur in units that otherwise display low black shale proportions. For example, the Roper Group (1.5 Ga) has a black shale proportion of 0.2. Within the Roper Group, a significant fraction of basinal shales have low S/C ratios (Donnelly & Crick 1988) and low DOP and Fe_{HR}/Fe_T values (Shen et al. 2003). Shen et al. (2003) interpret these apparently noneuxinic shale compositions as the result of Fe limitation or clastic dilution, but an alternative interpretation is that euxinia was an episodic rather than persistent feature. Clearly, additional analysis of the many other Proterozoic shale localities is needed to further support or refute Proterozoic global euxinia.

The Phanerozoic

The Phanerozoic record contains numerous examples of euxinic environments. Because Paleozoic sections are heavily biased toward cratonic basins that record shallow epicontinental (epeiric) sea deposition, the spatial and temporal extent of free sulfide in the ocean is often unclear. Euxinic sediments have been associated with

several episodes of mass extinction, including the Late Ordovician, the Frasnian-Famennian, and the Permo-Triassic (see below). Furthermore, the well-known Cretaceous oceanic anoxic events host abundant evidence for sulfide in the water column. Interestingly, there are relatively few indications of widespread water column euxinia during the Cenozoic.

The Paleozoic. The long-lived Selwyn Basin of the Canadian Yukon experienced several episodes of anoxic and euxinic deep waters during the Paleozoic (Goodfellow & Jonasson 1984). In the Early Silurian (Llandoverian), Early Devonian, and Middle to Late Devonian, the $\delta^{34}S$ of hydrogen sulfide (reflected in pyrite) came to exceed that of sulfate (reflected in preserved barite). Although Goodfellow & Jonasson (1984) explain these isotope anomalies by invoking local tectonic factors to restrict circulation, we now recognize that this interval of time likely had low seawater sulfate concentrations, 5 to 10 mM (Horita et al. 2002, Lowenstein et al. 2003), when compared to a modern average of 28 mM. Thus, intense sulfate reduction and the establishment of basinal euxinia likely depleted the water column of sulfate.

More widespread evidence for basinal euxinia is especially prevalent in the Devonian and early Mississippian. Bioturbated sediments from the Devonian-Mississippian New Albany shales consistently have smaller C_{org}/P_{org} values (~150) than laminated shales (~3900) (Ingall et al. 1993). Kellwasser horizons (Frasnian/Famenian) from New York State have greatly increased C_{org}/P_{org} ratios, increasing from ~100 to ~5000 in the black shales (Murphy et al. 2000, Murphy et al. 2001). Isorenieratene derivatives have been isolated from black shales from the Illinois and Michigan basins spanning this age range (Brown & Kenig 2004). Interestingly, the sediments from which this biomarker was extracted are highly bioturbated, consistent with other indications that euxinia was an ephemeral feature of these basins (Schultz 2004). Sea-level fluctuations may have driven some variability, and have been invoked to explain high DOP, Fe/Ti, and Mo/Ti ratios of sediments in the Oatka Creek Formation of the Devonian Appalachian Basin during sea-level highstands (Werne et al. 2002). The cause for anoxia is thought to be thermal stratification followed by anoxic productivity feedbacks. The link between high sea level and thermal stratification remains unclear. Other indications of euxinia during Devonian to Mississippian times include the New Albany Shale of Indiana (Ripley et al. 1990), the classic Frasnian/Famennian Kellwasser events of the Holy Cross Mountains of Poland (Bond et al. 2004), and the lower Mississippian Sunbury Shale of Kentucky (Rimmer 2004).

The Permian. The Permian-Triassic (P-T) transition marks the largest extinction episode in the Phanerozoic. Many hypotheses for end-Permian extinction include the influence of ocean anoxia (Wignall & Twitchett 2002) because boundary sections from both the Tethys and Panthalassic oceans contain abundant evidence for deposition in low-oxygen conditions. Evidence for oceanic anoxia coincides with Pangean supercontinent formation, massive Emeishan and Siberian trap volcanism, and a seemingly global pause in coal deposition (Berner 2002). Global warmth in an ice-free world, elevated pCO_2, and low atmospheric pO_2 likely contributed to ocean anoxia and sulfide buildup in the deep ocean.

Deep Panthalassic sediments from modern Japan and British Columbia display sedimentological and geochemical evidence for a long period (nearly 20 Ma) of dysoxic to anoxic deposition punctuated by an interval of euxina at the P-T boundary (Isozaki 1997). Evidence for sulfide in the water column at the end-Permian comes from framboidal pyrite size distributions within both deep Panthalassic and shallow-water Tethys sections (Nielsen & Shen 2004, Wignall et al. 2005). In addition to sulfide mineral evidence of a sulfidic water column, the molecular fossil record documents photic-zone euxinia during the mass extinction interval in both the classic Meishan, China section and in core material from Western Australia (Grice et al. 2005). Furthermore, massive perturbations of the global sulfur and carbon cycles are documented by remarkable sulfur and carbon isotope variations. The $\delta^{34}S$ record from carbonate-associated sulfate may provide further evidence of periodic chemocline upward excursions during this mass extinction interval (Newton et al. 2004, Riccardi et al. 2006).

Not all P-T boundary sections display evidence for euxinia. For example, early Triassic marine faunas from central Oman do not display the common sulfide mineral precipitates and delayed biotic recovery that are characteristic of this time interval; instead, this site is free of evidence for anoxia/euxinia and this section exhibits a much more rapid recovery from extinction (Twitchett et al. 2004). How do we reconcile this section with evidence for anoxia, euxinia, and photic zone euxinia during the P-T interval?

Kump et al. (2005) used a simple numerical model to demonstrate that chemocline upward excursions can inject sulfide into the surface ocean and atmosphere as a consequence of realistic ocean and atmosphere conditions. In this scenario, warm deep-water source regions, decreased pO_2, and increased oceanic nutrient conditions enhance euxinia within a vigorously circulating ocean. Sulfide release from the euxinic ocean occurs when the upwelling flux of sulfide to the surface exceeds the downward mixing flux of oxygen from the atmosphere. Thus, the prediction is that upwelling areas would exhibit shallow-water euxinia, whereas stable oceanic gyre regions would retain an oxygenated wind-mixed layer. The deep ocean, however, would be globally euxinic. Unfortunately, definitive tests of this suggestion (e.g., Mo isotopic analysis) have yet to be performed.

Mesozoic oceanic anoxic events. OAEs were first described by Schlanger & Jenkyns (1976) as brief intervals of black shale deposition that are often accompanied by a carbon isotope excursion (Leckie et al. 2002). These laminated organic-rich sediments are thought to result from a combination of high primary productivity, enhanced preservation, and decrease in bulk accumulation rate. Considerable debate remains concerning the relative importance of these processes. Global causes of OAEs include the role of sea-level change, tectonism or volcanism, ocean circulation patterns, and global climate (Arthur & Sageman 1994, Leckie et al. 2002). Despite the expectation that global anoxic events might lead to euxinic conditions, the evidenciary linkages between OAEs and euxinia are based largely on molecular fossils within black shales (**Table 2**).

Black shale deposition during the Toarcian (Early Jurassic) OAE was widespread and associated with large $\delta^{13}C$ fluctuations. Me, *i*-Bu maleimides derived from anoxygenic sulfur phototrophs are observed in sediments from the Umbria-Marche Basin, Italy, which was on the continental margin of the Tethys during the Toarcian (Pancost et al. 2004). Isorenieratane and chlorobactane from the Posidon Shale (Germany) also support that this region experienced a shallow photic-zone euxinia (PZE) (Schouten et al. 2000). However, the Posidon Shale was deposited in an epicontinental basin that was intermittently open to both the Tethys and Arctic oceans. Finally, N isotope profiles through the Toarcian support the interpretation of strong denitrification rates within an anoxic water column (Jenkyns et al. 2001).

PZE: photic-zone euxinia

Denitrification: the microbial metabolic process whereby microorganisms convert nitrate to N_2

The early Aptian (late Early Cretaceous) oceanic anoxic event (OAE1a) may be associated with increased primary productivity and hypothesized increases in the efficiency of the biological pump (Leckie et al. 2002). Organic-rich sediments are preserved throughout the Tethys Ocean region; $\delta^{13}C$ measurements, absent bioturbation, and biotic turnover support deposition under an anoxic water column. Roughly coeval sediments from the Shatsky Rise in the Pacific Ocean also record carbon-rich deposition, with C/S ratios consistent with euxinic conditions (Dumitrescu & Brassell 2006). Maleimide molecular fossils identified in black shales of the Livello Selli are the first evidence for PZE during the Aptian OAE1a (Pancost et al. 2004).

The Cenomanian-Turonian (C-T) OAE2 (early Late Cretaceous) is distinguished by widespread black shale deposition worldwide with the greatest C_{org} accumulation observed in the proto–North Atlantic Ocean. Me, *i*-Bu maleimides have been identified in the Tethys, the North Atlantic, and the Indian oceans (Pancost et al. 2004). Similarly, sections throughout the North Atlantic contain GSB-derived isorenieratane, consistent with maleimide evidence for PZE (Damste & Koster 1998, Kuypers et al. 2002). Moroccan black shales show an increase in C_{org}/P_{tot} from 165 to an average of ~860 during OAE2 (Nederbragt et al. 2004). Detailed stratigraphic analysis of OAE2 reveals that the onset of anoxia/euxinia as revealed in the increase of C_{org}/P_{tot} followed a period of elevated productivity and P_{org} accumulation that presumably led to dysoxia in bottom waters (Mort et al. 2007). Finally, nitrogen isotopes from the Demerara Rise likely reflect N fixation, which might be expected in an anoxic ocean with N-depleted surface waters (Junium & Arthur 2007).

Although OAE black shales display abundant evidence for dysoxic and anoxic deposition, evidence of euxinia is not ubiquitous. Perhaps during these OAE intervals euxinia was more widespread, but photic zone euxinia may have been restricted to open ocean upwelling zones and isolated, silled, or restricted basins.

CAUSES OF EUXINIA

Observations of modern euxinic basins weigh heavily on most interpretations of ancient marine euxinia. Although these modern euxinic systems, such as the Black Sea, meromictic lakes, and fjords, share many biogeochemical characteristics with ancient euxinic water columns, there is no doubt that the physical and dynamical differences are enormous between small modern basins and vast ancient oceans. Attempting to

explain geological evidence of euxinia in the rock record, numerous authors invoke a range of causations to drive the oceans euxinic that include changes in ocean circulation, global climate, sea level, geography, and ocean nutrient status. A complicated interplay of factors likely contributes to euxinia; here we discuss the range of proposed scenarios and attempt to elucidate the forcings that are the primary cause of this unusual ocean state.

Ocean Stagnation

Ocean stagnation, a decrease in the overturning circulation, is often invoked to explain the occurrence of widespread black shales and euxinic conditions in Earth history (e.g., Fischer & Arthur 1977, Ryan & Cita 1977, Bralower & Thierstein 1984, Gruszczynski et al. 1992). It is often presumed that chemical stratification (strong redox and isotopic gradients) requires sluggish ocean circulation. The Black Sea analogue is the source of this presumption, although it is not a particularly appropriate model for ancient euxinic oceans (Arthur & Sageman, 1994). Of course, the modern ocean is simultaneously strongly stratified and vigorously mixed. Modern ocean chemical stratification is a consequence of intense biological pumping of nutrient-rich organic matter to the deep sea, which is only made possible by the continued supply of upwelling nutrients to the surface ocean (Sigman & Haug 2003).

In places such as the Black Sea, deep saline waters are trapped behind sills and overlain by fresher waters. This condition creates a stable density stratified water column, resistant to wind mixing, and thus with long deep-water residence times. Is the resistance to vertical mixing a dominant control on the water column structure of density stratified environments? Other parameters of interest include nutrient supply and the position of the chemocline. We use simple calculations to explore the relative importance of these factors for the genesis of a euxinic basin.

Using an approach similar to Kump et al. (2005), we quantify the relationship between overturning (u in meters per year), $[PO_4]$, $[H_2S]$ in the deep ocean, and $[O_2]$ in the surface ocean. The surface ocean box produces organic matter through photosynthesis; the deep ocean box consumes organic matter, remineralizes phosphate, and produces H_2S. We assume no P or H_2S in the surface ocean, no P removal via burial, and that O_2 generated from photosynthesis is small relative to wind mixing fluxes of O_2. Additionally, we remineralize C_{org} only in the deep layer. In this scenario, $[O_2]_{surf}$ is a function of wind mixing with atmospheric pO_2 (treated as a piston velocity), reaction with upwelled H_2S, loss through advection into the deep box, and is described by the equation

$$\partial[O_2]_{surf}/\partial t = K_H\, k\, pO_{2\ air}/dz_{surf} - K_H\, k\, pO_{2\ water}/dz_{surf} - u[O_2]_{surf}/dz_{surf} - 2u[H_2S]_{deep}/dz_{surf},$$

where K_H is the Henry's Law constant for O_2 and k is the piston velocity. The relative sizes of the deep ocean and surface ocean are defined by dz_{surf} and dz_{deep}.

$[H_2S]_{deep}$ is controlled by oxidant demand in the deep water, the downwelling flux of oxygen from the oxygenated surface layer, and H_2S advection into the surface

layer. Oxidant demand is related to surface-water productivity, which is limited by the upwelling flux of phosphate; the rate of H_2S production is determined by the Redfield ratio ($R = 106$) and the stoichiometry of sulfate reduction. The resulting description of the time rate of change of $[H_2S]_{deep}$ in the deep ocean is

$$\partial[H_2S]_{deep}/\partial t = 0.5\,R\,u[PO_4]_{deep}/dz_{deep} - u[H_2S]_{deep}/dz_{deep} - 0.5u[O_2]_{surf}/dz_{deep}.$$

At steady state,

$$[H_2S]_{ss,\ deep} = 0.5\,(R[PO_4]_{deep} - [O_2]_{ss,surf}) \text{ and}$$
$$[O_2]_{ss,\ surf} = -u\,R\,[PO_4]_{deep} + K_H\,k\,pO_{2\,air}.$$

Note that chemocline position does not affect the steady-state condition. If we take the partial derivatives of $[O_2]_{ss}$ and $[H_2S]_{ss}$ with respect to u, we find that

$$\frac{\partial[O_2]}{\partial u} = \left(\frac{-106}{k}\right)\cdot[PO_4] \text{ and}$$
$$\frac{\partial[H_2S]}{\partial u} = \left(\frac{53}{k}\right)\cdot[PO_4]$$

Interestingly, these equations reveal that as upwelling rate increases, $[O_2]_{ss,surfs}$ decreases, $[H_2S]_{ss,deep}$ increases, and the $[PO_4]$ required to generate euxinia diminishes. That is, to the extent that this simple model is an appropriate representation of a euxinic basin, not only is stagnation not required for euxinia, it is antithetical to euxinia. The euxinic basin model of Shen et al. (2002), although of somewhat different construction, leads to essentially the same conclusion.

Results from more sophisticated numerical models also demonstrate that ocean stagnation cannot induce euxinia. In stagnant oceans, the supply of nutrients to the surface ocean is insufficient to sustain the elevated productivity required to support high O_2 demand in the deep ocean (e.g., Hotinski et al. 2001). Sluggish oceans do result in significantly decreased oxygen supply; however, the reduction in oxygen flux to the deep ocean is balanced by reduction in oxygen demand. Further, global ocean simulations demonstrate that the thermohaline circulation rate can vary, but within limits that do not include stagnation. Even in the extreme case of an isothermal isohaline sea surface, heat flow from the seafloor will eventually drive convective overturning that mixes the ocean in approximately 15,000 years (Worthington 1968).

Nutrient Trapping and Estuarine Circulation

If stagnation is not a factor in the development of euxinic conditions, then how do we explain euxinia in modern systems? Perhaps a more important characteristic of these stratified bodies is that they are effective nutrient traps. Stanley (1978) championed the idea of a switch from estuarine to antiestuarine circulation in the Mediterranean as the primary cause of the Mediterranean sapropels. In this scenario, interglacial

episodes were marked by antiestuarine circulation generating a nutrient desert via surface-water import and deep-water export. A moist climate in the Mediterranean region during glacial intervals, Stanley argued, reversed the flow and accumulated nutrients without the need for more sluggish ocean circulation. Estuarine circulation is implicated in explanations for anoxia or euxinia in many basins (Demaison & Moore 1980).

The above observations raise the question of whether certain continental configurations are capable of creating vast nutrient-trapping areas, so that periods with "just right" geographies are conditioned for euxinia. As such, we used the GENIE model (Ridgwell et al. 2007) to examine the geography-nutrient trap link. Using modern, Paleocene-Eocene, Cretaceous (Cenomanian), and end-Permian continental configurations, we performed steady-state simulations with modern atmospheric and nutrient conditions. The nutrient-trapping efficiency for these configurations plus a generic "box world" geography with no nutrient traps are shown in **Figure 2**.

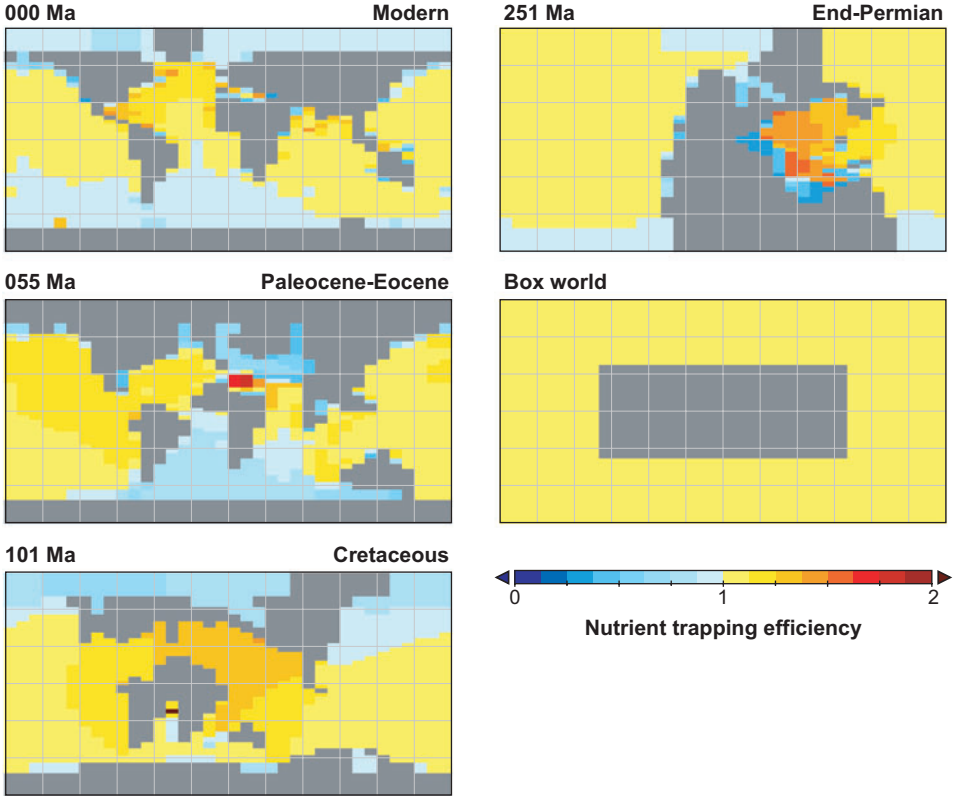

Figure 2

Nutrient trapping efficiency of various paleogeographic reconstructions based on model simulations of biogeochemical cycling using the GENIE Earth system model. Efficiency factors are the ratio of phosphate concentration to the global average phosphate concentration.

We define nutrient trapping efficiency as the ratio of the $[PO_4]_{deep}$ of a region to the global average $[PO_4]_{deep}$. The value ranges from 0.3 to 1.8 for the different scenarios. Although the four other time periods exhibit similar ranges in nutrient trapping efficiency, the end-Permian configuration has the greatest areal extent of nutrient trapping. It appears that geography, which influences nutrient trapping efficiency and spatial extent of nutrient trapping regions, plays a role in predisposing areas to euxinic conditions. However, based on our earlier establishment of $[PO_4]_{deep} = 4\ \mu M$ as a threshold for euxina and a modern average $[PO_4]_{deep}$ of 2.2 μM, a nutrient trapping efficiency of 1.8 would be just sufficient for euxinia. This finding is consistent with the dearth of euxinic marine basins today, and suggests that global phosphate inventories must have been significantly elevated during the mid-Cretaceous, latest Permian, Late Devonian, and, perhaps, the Proterozoic, times for which euxinia seems to have been widespread.

Sea Level

Basin morphology changes with sea level and can influence circulation patterns and nutrient-trapping efficiency. For example, the water depth over a basin sill changes with sea level and can have profound effects on the nutrient regime of a basin. Arthur & Sageman (2005) invoke sea level transgression to explain Cenomanian-Turonian oceanic anoxia. In this situation, deeper sill depths allow nutrient-rich deep water to enter basins with estuarine circulation, leading to eutrophication and anoxia. The rock record is biased toward preservation of such cratonic/epicontinental depositional environments, so circulation-induced nutrient trapping and consequent euxinia may be disproportionately recorded.

Do most euxinic intervals occur predominantly during sea-level highstands? Despite controversy concerning the magnitude of sea-level change, the end Devonian and Cretaceous appear to occur during relative highstands (Miller 2005). However, the end-Permian is a notable exception, where widespread evidence for euxinia coincides with an extreme lowstand. Geographical qualities, including water depth and circulation pattern, certainly seem to influence euxinia via changes in nutrient dynamics, although it does not fully account for the occurrence of euxinia.

Global Warming

Oxygen solubility is temperature dependent, so warmer sea surface temperatures in deep-water-forming regions should lead to less oxygen supply to the deep ocean. Schlanger & Jenkyns (1976) and Fischer & Arthur (1977) invoked the warm, equable Cretaceous climate in suggesting that the high latitudes were probably not good sources of oxygen-rich water for the world ocean, which, together with higher productivity, caused the expansion of the oxygen minimum zone (OMZ) during oceanic anoxic events. Herbert & Sarmiento (1991) used an ocean box model to argue that a shift to warm, salty bottom waters would favor anoxia owing to increased biological pump efficiency. Ocean general circulation modeling studies (e.g., Hotinski et al. 2001) confirm that the key link between warm climates and anoxia/euxinia is the reduced solubility of oxygen in warmer deep-water source regions and the

improved ability of high-latitude-dwelling plankton to exploit nutrients (Sarmiento et al. 1988).

Not only does global warmth reduce deep-water [O_2], it also stimulates the hydrologic cycle and weathering rates of continental rocks, which in turn increases the supply of nutrients (e.g., phosphate) to the ocean. An increase in phosphate supply leads to higher primary productivity, which increases the O_2 demand in deep water via an increased C_{org} flux to the deep ocean (i.e., enhanced export productivity), creating a positive feedback loop.

Do warm climates indeed coincide with euxinic intervals? Many of the euxinic intervals identified in this review are linked to global warmth. For example, the end-Permian is widely considered to be a time of global warmth (e.g., Kiehl & Shields 2005). Euxinia during the Frasnian-Famennian transition, another euxinic interval concurrent with mass extinction, occurred during the transition from the global warmth of the Devonian to Carboniferous glaciation, but may have been associated with a short-term warming (Kaiser et al. 2006). The mid-Cretaceous is a notable greenhouse interval, and intermittent euxinia is dispersed throughout (Pancost et al. 2004). The Proterozoic also lacks glacial evidence between 2.2 and 0.75 Ga, suggestive of a warm climate. As pointed out above, the detailed nature of the Proterozoic ocean redox state and its link to climate remains unresolved.

Conceptual Model for Widespread Oceanic Euxinia

We conclude that climate and nutrient-trapping geography are the two ultimate constraints on the redox state of the world oceans (see also Arthur & Sageman 2005). Widespread euxinia, especially the extreme state leading to mass extinction, seems to have occurred when the climate was warm, but only in basins that were predisposed to euxinia because of efficient nutrient trapping.

We might best express this conclusion in the form of a systems diagram displaying the various forcing factors and feedback loops involved (**Figure 3**). The central external trigger for euxinia is proposed to be enhanced volcanism (release of volcanic CO_2), although other external forcings of the climate system could be imagined (changing solar luminosity, changes in continental configuration affecting ocean circulation or the stability of ice sheets, etc.). The resulting increase in atmospheric pCO_2 leads to global warming, an intensification of continental weathering, and enhanced delivery of nutrients to the ocean. This weathering-derived stimulation of ocean export productivity combines with decreased O_2 delivery to the deep ocean as a result of solubility-temperature relationships to further reduce oxygen content of the deep water. Sulfide produced from bacterial sulfate reduction appears once oxygen is depleted. Subsequent reducing conditions liberate iron-sorbed phosphate from sediments, further increasing nutrient fluxes to the surface (Ingall et al. 1993). Nutrient traps amplify this increase in phosphate concentration to create highly eutrophic basins with elevated hydrogen sulfide concentrations. Burial of phosphate is minimal under reducing conditions, so phosphate concentrations remain high for a geologically significant period of time. The positive feedback loop represented by

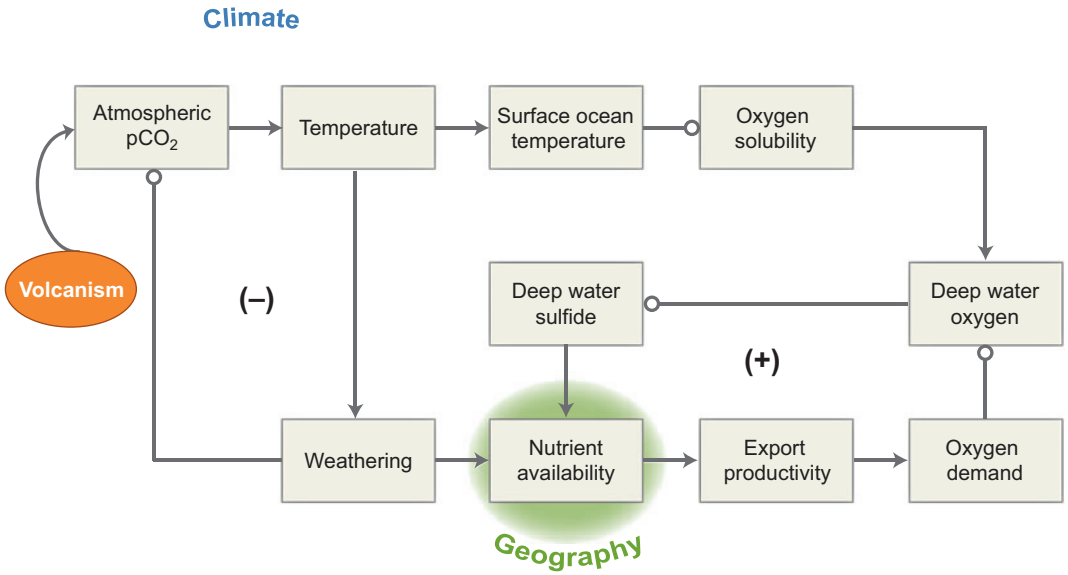

Figure 3

Systems diagram displaying the components involved in the establishment and maintenance of euxinia in the world ocean and feedbacks among them. Linkages are either positive (*normal arrow*), indicating that the response is in the same direction, or negative (*circular arrow head*), indicating that the response is in the opposite direction. For example, an increase in temperature causes an increase in weathering, but increased weathering causes a decrease in atmospheric pCO_2.

these processes and the resultant euxinia persists until the forcing (volcanism) ceases, at which point the pCO_2-weathering feedback begins to cool the climate and slowly bury phosphate. Alternatively, a buildup of atmospheric oxygen stimulated by enhanced organic carbon burial under euxinic conditions and elevated C/P ultimately causes an oxygenation of the deep ocean despite its warmth and elevated nutrient content (Van Cappellen & Ingall 1996). Thus, both global (climate) and regional (basin geography and mode of circulation) factors play a role, but ultimately it is the phosphate concentration of basinal waters that determines the extent of euxinia in a particular basin.

THE TRANSITION TO EUXINIA

The transition of an ocean basin from either an anoxic (Late Archean) or an oxic (Phanerozoic) to a euxinic state involves passage through an intermediate state where denitrification dominates organic-matter regeneration. Falkowski (1997) has argued that this creates a potential fixed-nitrogen crisis. Fe-limited nitrogen-fixing bacteria would not keep pace with denitrification, causing depletion of fixed nitrogen and placing severe constraints on ocean productivity. This crisis could be a driver for Late Devonian and Late Permian extinction as well as an explanation for the "boring

billion" years of the mid-Proterozoic [the interval of the Canfield Ocean (Anbar & Knoll 2002)] characterized by little variation in the carbon cycle, as inferred from the carbon isotope record (Kerr 2005, Holland 2006).

We note, however, that the soluble Fe concentration in euxinic deep waters of the Black Sea is as high as 300 nmol kg^{-1} (Yemenicioglu et al. 2006), two orders of magnitude higher than in the oxic deep waters of the modern global ocean; upwelling of these Fe-enriched waters to the surface would have provided an enhanced source of Fe to surface waters. Therefore, Fe limitation may not have been a major consequence of the Canfield Ocean. Additional worries about Fe-limitation of nitrogen fixation may also be quelled by Arrigo (2005), who suggests that the Fe demands of nitrogen fixing cyanobacteria are far less than previously estimated. Moreover, recent analysis of the distribution of nitrogen fixation and denitrification in the modern global ocean suggests strong spatial coupling (Deutsch et al. 2007) that would facilitate the homeostatic regulation of fixed nitrogen availability.

Simple but elegant box modeling by Fennel et al. (2005) supports the suggestion that denitrification during the oxidation of the Proterozoic ocean caused widespread nitrogen limitation and dramatically decreased primary productivity. However, the model specifies a very low phosphate inventory for the anoxic/euxinic ocean (0.2 μM), whereas one might expect that anoxic/euxinic oceans would instead be enriched in phosphate and thus able to support high rates of nitrogen fixation.

For these reasons, we conclude that the transition to the euxinic state would likely occur without severe nutrient limitation. The transition is driven by phosphate accumulation and is matched by a near-stoichiometric ammonium accumulation in the deep sea. Deep-water nitrate concentrations decline because of enhanced denitrification in intermediate waters. The reduced supply of nitrate to the euphotic zone provides a competitive advantage to N_2-fixing phototrophs. Export of biologically fixed nitrogen to the deep sea continues without substantial reduction, providing a source of ammonium to the deep sea via anaerobic remineralization.

Nevertheless, nitrate is reduced before sulfate in an anoxic ocean, and so a continuous supply of fixed nitrogen could substantially delay the onset or intensity of sulfidic conditions compared with what one might conclude based on a consideration of phosphate-oxygen-sulfate cycling alone. Further field and computational studies are needed to detail the role of the N cycle during the transition to euxinia.

EUXINIA AND MASS EXTINCTION

The episodic development of euxinia documented here may have placed significant stress on marine communities during particular intervals of Earth history. Although many organisms have defense mechanisms for dealing with brief exposure to H_2S (Bagarinao 1992), persistent euxinia would have created intolerable conditions for all aerobic organisms. Sulfide would first appear in the oxygen minimum zone (~1 km depth) and initiate disruption of continental slope benthic communities. As this toxic zone expanded to the seafloor with increasing eutrophication of the ocean, deep-sea animal communities would have been annihilated because of lack of refugia; unfortunately, there is no fossil record to test this assertion. What we know is that

at times in Earth history, notably the Late Ordovician, Late Devonian, and Late Permian, widespread shelf and cratonic-basinal anoxia, and, at least in the latter two cases, photic-zone euxinia, have accompanied mass extinction (Wilde & Berry 1984; Wignall & Hallam 1992; Wang et al. 1993, 1996; Bond et al. 2004). Could sulfide poisoning serve as the kill mechanism in these extinctions?

Wilde & Berry (1984) and Wang et al. (1993) have called on exposure of shallow-water-dwelling aerobic organisms to toxic deep waters in their explanations for the Late Ordovician mass extinction. This event is inexorably linked with Gondwanan glaciation, with extinction occurring in two phases, one associated with the onset of glaciation and the other with the end of glaciation (Sheehan 2001). In contrast to the euxinia model above, Wilde & Berry (1984) invoke cooling after a long interval of global warmth to destabilize a highly stratified water column that has become toxic through anoxia and lack of biological conditioning. Toxic waters are mixed to the surface and impinge on shelf communities, causing widespread death and, in some cases, extinction. This destabilization ultimately leads to oxygenation of deep waters, but presumably surface waters become enriched in hydrogen sulfide and toxic metals during the transition. Moreover, oxygenation could stress organisms, such as graptolites, adapted to live under the low-oxygen conditions of the chemocline (Sheehan 2001).

Biomarker evidence perhaps provides a more compelling link between euxinia and extinction for the Late Devonian and Late Permian (Grice et al. 2005). These extinctions were widespread, affecting shallow-water marine ecosystems as well as Permian terrestrial ecosystems. In the marine realm, persistent deep-water euxinia could gradually draw down the oceanic inventory of essential trace elements (e.g., Mo and Cu), leading to widespread reductions in biological productivity (Anbar & Knoll 2002) and, ultimately, extinction. But why would a collapse of marine productivity trigger terrestrial ecosystem disruption and extinction?

Kump et al. (2005) proposed a more direct link between terrestrial and marine extinction in which sulfidic chemocline waters invade the surface ocean. These chemocline upward excursions would occur spontaneously once deep-water H_2S concentrations exceeded a critical concentration determined by the vigor of wind mixing, upwelling rate, and the atmospheric O_2 partial pressure. Once the wind-mixed layer of the ocean became euxinic, H_2S would escape to the atmosphere, and, depending on the flux, toxic levels of atmospheric H_2S could accumulate. Of course, it is highly unlikely that the entire surface ocean would become euxinic at these times. The stable subtropical oceanic gyres where downwelling prevails would likely remain oxygenated. Sulfidic surface waters would be restricted to regions of strong oceanic or coastal upwelling or shallow-water nutrient traps, where extremely sulfidic bottom waters would be developed (Kump et al. 2005). The patchy nature of euxinia means that marine refugia would exist under even highly euxinic global conditions, but would be limited to low-productivity gyres or the boundaries of highly productive (but highly toxic) upwelling regions. Thus, for the marine realm, we would predict that extinction would be the result of chronic stress over several generations of various lineages rather than an acute stress of a sudden environmental change (Bambach 2006).

Sulfide release from the oceans serves as a link to terrestrial biotic crisis during the end-Permian. One-dimensional atmospheric modeling by Kump et al. (2005) predicted that toxic levels of H_2S could rapidly accumulate in the well-mixed troposphere once reaction of sulfide with atmospheric hydroxyl radical reduced OH to very low levels. The abrupt rise in atmospheric H_2S concentrations would be accompanied by rising atmospheric methane levels and destruction of the ozone layer. Not only would terrestrial organisms be unable to escape the toxic effects of H_2S, but they also would be subject to high levels of UV radiation following the predicted collapse of the ozone layer.

This scenario is consistent with preliminary evidence for elevated sulfur inputs to terrestrial ecosystems, including sulfur enrichments in lacustrine sediments (Newton et al. 2007) and paleosols (G. Retallack, personal communication). However, more sophisticated three-dimensional modeling of the atmosphere has shown that if the critical air-sea H_2S flux identified by us exists, it occurs at fluxes higher than 4000 Tg S $year^{-1}$ (Lamarque et al. 2007). Perhaps rather than persistently toxic levels of H_2S in the atmosphere (as predicted by Kump et al. 2005), patches of H_2S-rich air could have wafted across the continents as discrete events, separated by longer intervals during which H_2S was at a stressful, but nontoxic, lower level.

Low or fluctuating concentrations of H_2S in surface waters, and temporally variable atmospheric H_2S levels, would also present a more selective killer. Although H_2S is generally toxic, marine organisms show a wide range of sensitivity and adaptations that reflect their typical level of exposure to H_2S. For example, infaunal organisms (burrowing invertebrates) can tolerate extended exposure to H_2S, whereas sessile organisms in highly oxygenated settings (e.g., corals) and many fish are highly sensitive to even low levels of H_2S (Bagarinao 1992). Thus, H_2S, together with its inseparable biogeochemical partner CO_2, could explain the apparent selection against poorly ventilated, sessile marine invertebrates during the end-Permian mass extinction (Knoll et al. 1996, Bambach 2006).

We also observe many euxinic intervals in Earth history that are not accompanied by an extinction event. Even during times of biotic crisis the pattern of extinction differs, suggesting the primary forcing differed between events. What factors separate these most-lethal extinction events from other euxinic intervals? Perhaps the spatial extent and exposure time to sulfidic waters are critical variables in causing extinction versus local die-off. For example, abundant evidence at the end-Permian suggests that much of the Tethys Ocean and at least multiple regions of the deep Panthalassic were sulfidic. This evidence is coincident with the largest of the mass extinctions, and selectivity of extinction could be explained by H_2S or CO_2 toxicity. In other records, biomarkers indicative of euxinia can be isolated from fossiliferous or bioturbated sediments (Kenig et al. 2004). This observation suggests that euxinic conditions were dynamic and episodic in many ancient basins. Moreover, the isolated euxinic basins today do not exert selective pressures that might lead to extinction. It is possible that many ancient oceans were similar to the modern, where euxinic conditions are restricted to a few isolated basins or occur only periodically in upwelling areas. During these times we would not expect euxinia-related extinction.

SUMMARY POINTS

1. Modern euxinic environments are the result of efficient nutrient trapping, not stagnant circulation leading to poor oxygen supply.
2. Most proxies for euxinia in ancient sediment are nondiagnostic, thus multiple proxy methods should be used. The presence of biomarkers for photic zone euxinia is likely diagnostic if the biomarkers can be shown to be autochthonous.
3. Euxinia was absent from the Archean because of the low availability of sulfate on the anoxic Earth. Proterozoic euxinia is well represented in the rock record, but may not have been a global and persistent feature for the duration of the Proterozoic era. The same can be said for the Paleozoic and Mesozoic.
4. The necessary conditions for widespread oceanic euxinia seem to be a high oceanic inventory of nutrient phosphate and a paleogeography that creates abundant nutrient traps. The buildup of oceanic phosphate occurs during greenhouse climate intervals because of lower oxygen supply to the deep sea, release of phosphate from sediments under anoxic conditions, and enhanced continental weathering.
5. Transitions to the euxinic state did not involve crises in the availability of fixed nitrogen; nitrogen fixation was likely able to keep up with enhanced denitrification as oceanic oxygen minimum zones expanded.
6. Hydrogen sulfide, together with its biogeochemical partner carbon dioxide, likely played a prominent role in mass extinctions during the Late Devonian and Late Permian, and perhaps during the Late Ordovician and other Phanerozoic mass extinctions.

FUTURE ISSUES

1. The search for proxy evidence of euxinia in Proterozoic rocks should be expanded beyond the heavily studied sites reported to date to evaluate the geographic extent and temporal persistence of euxinia during this critical interval of Earth history.
2. A focus of this work should be the establishment of a secular curve for the Mo isotopic composition of seawater for the Proterozoic and Phanerozoic.
3. Coupled ocean-atmosphere models including ocean biogeochemistry, capable of simulating anoxic/euxinic ocean basins, should be developed and applied to the problem of the global controls of euxinia, the spatial extent of photic-zone euxinia, and the nature of the transition to euxinia.

DISCLOSURE STATEMENT

L.R.K. received funding from the U.S. National Science Foundation to study oceanic euxinia.

ACKNOWLEDGMENTS

K.M.M. acknowledges support from the PSU-NSF BRIE IGERT (DGE 9972759) and the PSU Krynine Fund. L.R.K. and K.M.M. acknowledge support from the NSF Geobiology and Environmental Geochemistry program (EAR 0208119) and the NASA Astrobiology Institute (NNA04CC06A).

LITERATURE CITED

Algeo TJ. 2004. Can marine anoxic events draw down the trace element inventory of seawater? *Geology* 32:1057–60

Algeo TJ, Lyons TW. 2006. Mo-total organic carbon covariation in modern anoxic marine environments: implications for analysis of paleoredox and paleohydrographic conditions. *Paleoceanography* 21(1):PA1016

Algeo TJ, Maynard JB. 2004. Trace-element behavior and redox facies in core shales of Upper Pennsylvanian Kansas-type cyclothems. *Chem. Geol.* 206:289–318

Anbar AD, Knoll AH. 2002. Proterozoic ocean chemistry and evolution: a bioinorganic bridge? *Science* 297:1137–42

Anderson LG, Dyrssen D, Hall POJ. 1988. On the sulfur chemistry of a super-anoxic fjord, Framvaren, south Norway. *Mar. Chem.* 23:283–93

Arnold GL, Anbar AD, Barling J, Lyons TW. 2004. Molybdenum isotope evidence for widespread anoxia in mid-Proterozoic oceans. *Science* 304:87–90

Arrigo KR. 2005. Marine microorganisms and global nutrient cycles. *Nature* 437:349–55

Arthur MA, Sageman BB. 1994. Marine black shales: depositional mechanisms and environments of ancient deposits. *Annu. Rev. Earth Planet. Sci.* 22:499–551

Arthur MA, Sageman BB. 2005. Sea-level control on source-rock development: perspectives from the Holocene Black Sea, the mid-Cretaceous Western Interior Basin, and the late Devonian Appalachian basin. In *The Deposition of Organic-Carbon-Rich Sediments: Models, Mechanisms, and Consequences*, ed. NB Harris, *Spec. Pub. 82*, pp. 35–59. Tulsa, OK: SEPM. 282 pp.

Bagarinao T. 1992. Sulfide as an environmental-factor and toxicant—tolerance and adaptations in aquatic organisms. *Aquat. Toxicol.* 24:21–62

Bambach RK. 2006. Phanerozoic biodiversity and mass extinctions. *Annu. Rev. Earth Planet. Sci.* 34:27–55

Banerjee S, Dutta S, Paikaray S, Mann U. 2006. Stratigraphy, sedimentology and bulk organic geochemistry of black shales from the Proterozoic Vindhyan Supergroup (central India). *J. Earth Syst. Sci.* 115:37–47

Berner RA. 2002. Examination of hypotheses for the Permo-Triassic boundary extinction by carbon cycle modeling. *Proc. Natl. Acad. Sci. USA* 99:4172–77

Discussion of sea-level control on nutrient supply, primary productivity, and redox conditions during the formation of organic-rich shales.

Includes a review of the kill mechanisms proposed for the end-Permian extinction and relates them to fossil evidence.

Berner RA, Raiswell R. 1983. Burial of organic carbon and pyrite sulfur in sediments over Phanerozoic time: a new theory. *Geochim. Cosmochim. Acta* 47:855–62
Berner RA, Raiswell R. 1984. C/S method for distinguishing freshwater from marine sedimentary rocks. *Geology* 12:365–68
Bond D, Wignall PB, Racki G. 2004. Extent and duration of marine anoxia during the Frasnian-Famennian (Late Devonian) mass extinction in Poland, Germany, Austria and France. *Geol. Mag.* 141:173–93
Bralower TJ, Thierstein HR. 1984. Low productivity and slow deep-water circulation in mid-Cretaceous ocean. *Geology* 12:614–18
Brocks JJ, Love GD, Summons RE, Knoll AH, Logan GA, Bowden SA. 2005. Biomarker evidence for green and purple sulphur bacteria in a stratified Palaeoproterozoic sea. *Nature* 437:866–70
Broecker WS, Peng T-H. 1982. *Tracers in the Sea*. Palisades, NY: Eldigio Press. 690 pp.
Brown TC, Kenig F. 2004. Water column structure during deposition of Middle Devonian-Lower Mississippian black and green/gray shales of the Illinois and Michigan basins: a biomarker approach. *Palaeogeogr. Palaeoclim. Palaeoecol.* 215:59–85
Brumsack HJ. 2006. The trace metal content of recent organic carbon-rich sediments: implications for Cretaceous black shale formation. *Palaeogeogr. Palaeoclim. Palaeoecol.* 232:344–61
Brunskill GJ, Ludlam SD. 1969. Fayetteville Green Lake, New York. I. Physical and chemical limnology. *Limnol. Oceanogr.* 14:817–29
Calvert SE, Karlin RE. 1991. Relationships between sulfur, organic carbon, and iron in the modern sediments of the Black Sea. *Geochim. Cosmochim. Acta* 55:2483–90
Calvert SE, Thode HG, Yeung D, Karlin RE. 1996. A stable isotope study of pyrite formation in the Late Pleistocene and Holocene sediments of the Black Sea. *Geochim. Cosmochim. Acta* 60:1261–70
Canfield DE. 1998. A new model for Proterozoic ocean chemistry. *Nature* 396:450–53
Canfield DE, Poulton SW, Narbonne GM. 2007. Late-Neoproterozoic deep-ocean oxygenation and the rise of animal life. *Science* 315:92–95
Canfield DE, Raiswell R, Bottrell S. 1992. The reactivity of sedimentary iron minerals toward sulfide. *Am. J. Sci.* 292:659–83
Canfield DE, Teske A. 1996. Late Proterozoic rise in atmospheric oxygen concentration inferred from phylogenetic and sulphur-isotope studies. *Nature* 382:127–32
Condie KC, Des Marais DJ, Abbott D. 2001. Precambrian superplumes and supercontinents: a record in black shales, carbon isotopes, and paleoclimates? *Precambrian Res.* 106:239–60
Damste JSS, Kenig F, Koopmans MP, Koster J, Schouten S, et al. 1995. Evidence for gammacerane as an indicator of water column stratification. *Geochim. Cosmochim. Acta* 59:1895–900
Damste JSS, Koster J. 1998. A euxinic southern North Atlantic Ocean during the Cenomanian/Turonian oceanic anoxic event. *Earth Planet. Sci. Lett.* 158:165–73
Damste JSS, Schouten S, van Duin ACT. 2001. Isorenieratene derivatives in sediments: possible controls on their distribution. *Geochim. Cosmochim. Acta* 65:1557–71

Del Don C, Hanselmann KW, Peduzzi R, Bachofen R. 2001. The meromictic alpine Lake Cadagno: orographical and biogeochemical description. *Aquat. Sci.* 63:70–90

Demaison GJ, Moore GT. 1980. Anoxic environments and oil source bed genesis. *Am. Assoc. Pet. Geol. Bull.* 64:1179–209

Deutsch C, Sarmiento JL, Sigman DM, Gruber N, Dunne JP. 2007. Spatial coupling of nitrogen inputs and losses in the ocean. *Nature* 445:163–67

Donnelly TH, Crick IH. 1988. Depositional environment of the middle Proterozoic Velkerri Formation in Northern Australia: geochemical evidence. *Precambrian Res.* 42:165–72

Dumitrescu M, Brassell SC. 2006. Compositional and isotopic characteristics of organic matter for the early Aptian oceanic anoxic event at Shatsky Rise, ODP leg 198. *Palaeogeogr. Palaeoclim. Palaeoecol.* 235:168–91

Eggleton FE. 1931. A limnological study of the profundal bottom fauna of certain fresh-water lakes. *Ecol. Monogr.* 1:231–331

Falkowski PG. 1997. Evolution of the nitrogen cycle and its influence on the biological sequestration of CO_2 in the ocean. *Nature* 387:272–75

Fallesen G, Andersen F, Larsen B. 2000. Life, death and revival of the hypertrophic Mariager Fjord, Denmark. *J. Mar. Syst.* 25:313–21

Fennel K, Follows MJ, Falkowski PG. 2005. The coevolution of the nitrogen, carbon, and oxygen cycles in the Proterozoic ocean. *Am. J. Sci.* 305:526–45

Fike DA, Grotzinger JP, Pratt LM, Summons RE. 2006. Oxidation of the Ediacaran Ocean. *Nature* 444:744–47

Filippelli GM. 2001. Carbon and phosphorus cycling in anoxic sediments of the Saanich Inlet, British Columbia. *Mar. Geol.* 174:307–21

Fischer AG, Arthur MA. 1977. Secular variations in the pelagic realm. In *Deep-Water Carbonate Environments*, ed. HE Cook, P Enos, pp. 19–50. Tulsa, OK: SEPM

Gellatly AM, Lyons TW. 2005. Trace sulfate in mid-Proterozoic carbonates and the sulfur isotope record of biospheric evolution. *Geochim. Cosmochim. Acta* 69:3813–29

Goodfellow WD, Jonasson IR. 1984. Ocean stagnation and ventilation defined by $\delta^{34}S$ secular trends in pyrite and barite, Selwyn Basin, Yukon. *Geology* 12:583–86

Grice K, Cao CQ, Love GD, Bottcher ME, Twitchett RJ, et al. 2005. Photic zone euxinia during the Permian-Triassic superanoxic event. *Science* 307:706–9

Grice K, Gibbison R, Atkinson JE, Schwark L, Eckardt CB, Maxwell JR. 1996. Maleimides (1H-pyrrole-2,5-diones) as molecular indicators of anoxygenic photosynthesis in ancient water columns. *Geochim. Cosmochim. Acta* 60:3913–24

Gruszczynski M, Hoffman A, Malkowski K, Veizer J. 1992. Seawater strontium isotopic perturbation at the Permian-Triassic boundary, West Spitsbergen, and its implications for the interpretation of strontium isotopic data. *Geology* 20:779–82

Habicht KS, Gade M, Thamdrup B, Berg P, Canfield DE. 2002. Calibration of sulfate levels in the Archean ocean. *Science* 298:2372–74

Hartgers WA, Damste JSS, Requejo AG, Allan J, Hayes JM, et al. 1994. A molecular and carbon isotopic study towards the origin and diagenetic fate of diaromatic carotenoids. *Org. Geochem.* 22:703–25

Hays L, Love GD, Foster CB, Grice K, Summons RE. 2006. Lipid biomarker records across the Permian-Triassic boundary from Kap Stosch, Greenland. *Eos Trans. AGU* 87(52):PP41B–1203 (Abstr.)

Herbert TD, Sarmiento JL. 1991. Ocean nutrient distribution and oxygenation—limits on the formation of warm saline bottom water over the past 91 My. *Geology* 19:702–5

Holland HD. 2006. The oxygenation of the atmosphere and oceans. *Philos. Trans. R. Soc. B-Biol. Sci.* 361:903–15

Horita J, Zimmerman H, Holland HD. 2002. The chemical evolution of seawater during the Phanerozoic: implications from the record of marine evaporites. *Geochim. Cosmochim. Acta* 66(21):3733–56

Hotinski RM, Bice KL, Kump LR, Najjar RG, Arthur MA. 2001. Ocean stagnation and end-Permian anoxia. *Geology* 29:7–10

Huang YS, Freeman KH, Wilkin RT, Arthur MA, Jones AD. 2000. Black Sea chemocline oscillations during the Holocene: molecular and isotopic studies of marginal sediments. *Org. Geochem.* 31:1525–31

Imbus SW, Macko SA, Elmore RD, Engel MH. 1992. Stable isotope (C, S, N) and molecular studies on the Precambrian Nonesuch Shale (Wisconsin-Michigan, USA)—evidence for differential preservation rates, depositional environment and hydrothermal influence. *Chem. Geol.* 101:255–81

Ingall E, Jahnke R. 1997. Influence of water-column anoxia on the elemental fractionation of carbon and phosphorus during sediment diagenesis. *Mar. Geol.* 139:219–29

Ingall ED, Bustin RM, Van Cappellen P. 1993. Influence of water column anoxia on the burial and preservation of carbon and phosphorus in marine shales. *Geochim. Cosmochim. Acta* 57:303–16

Isozaki Y. 1997. Permo-Triassic boundary superanoxia and stratified superocean: records from lost deep sea. *Science* 276:235–38

Jackson MJ, Raiswell R. 1991. Sedimentology and carbon sulfur geochemistry of the Velkerri Formation, a Midproterozoic potential oil source in Northern Australia. *Precambrian Res.* 54:81–108

Jenkyns HC, Grocke DR, Hesselbo SP. 2001. Nitrogen isotope evidence for water mass denitrification during the early Toarcian (Jurassic) oceanic anoxic event. *Paleoceanography* 16:593–603

Johnston DT, Poulton SW, Fralick PW, Wing BA, Canfield DE, Farquhar J. 2006. Evolution of the oceanic sulfur cycle at the end of the Paleoproterozoic. *Geochim. Cosmochim. Acta* 70:5723–39

Johnston DT, Wing BA, Farquhar J, Kaufman AJ, Strauss H, et al. 2005. Active microbial sulfur disproportionation in the Mesoproterozoic. *Science* 310:1477–79

Junium CK, Arthur MA. 2007. Nitrogen cycling during the Cretaceous, Cenomanian-Turonian oceanic anoxic event II. *Geochem. Geophys. Geosyst.* 8:Q03002

Kah LC, Lyons TW, Frank TD. 2004. Low marine sulphate and protracted oxygenation of the Proterozoic biosphere. *Nature* 431:834–38

Kaiser SI, Steuber T, Becker RT, Joachimski MM. 2006. Geochemical evidence for major environmental change at the Devonian-Carboniferous boundary in the Carnic Alps and the Rhenish Massif. *Palaeogeogr. Palaeoclim. Palaeoecol.* 240:146–60

Kenig F, Hudson JD, Damste JSS, Popp BN. 2004. Intermittent euxinia: reconciliation of a Jurassic black shale with its biofacies. *Geology* 32:421–24

Kerr RA. 2005. Earth science: the story of O_2. *Science* 308:1730–32

Kiehl JT, Shields CA. 2005. Climate simulation of the latest Permian: implications for mass extinction. *Geology* 33:757–60

King C. 2004. *The Black Sea: A History*. New York: Oxford Univ. Press. 276 pp.

Knoll AH, Bambach RK, Canfield DE, Grotzinger JP. 1996. Comparative Earth history and Late Permian mass extinction. *Science* 273:452–57

Koopmans MP, Koster J, van Kaam-Peters HME, Kenig F, Schouten S, et al. 1996a. Diagenetic and catagenetic products of isorenieratene: molecular indicators for photic zone anoxia. *Geochim. Cosmochim. Acta* 60:4467–96

Koopmans MP, Schouten S, Kohnen MEL, Damste JSS. 1996b. Restricted utility of aryl isoprenoids as indicators for photic zone anoxia. *Geochim. Cosmochim. Acta* 60:4873–76

Kump LR, Pavlov A, Arthur MA. 2005. Massive release of hydrogen sulfide to the surface ocean and atmosphere during intervals of oceanic anoxia. *Geology* 33:397–400

Kuypers MMM, Pancost RD, Nijenhuis IA, Damste JSS. 2002. Enhanced productivity led to increased organic carbon burial in the euxinic North Atlantic basin during the late Cenomanian oceanic anoxic event. *Paleoceanography* 17(4):1051

Lamarque JF, Kiehl JT, Orlando JJ. 2007. Role of hydrogen sulfide in a Permian-Triassic boundary ozone collapse. *Geophys. Res. Lett.* 34:L02801

Leckie RM, Bralower TJ, Cashman R. 2002. Oceanic anoxic events and plankton evolution: biotic response to tectonic forcing during the mid-Cretaceous. *Paleoceanography* 17(3):1041

Lowenstein TK, Hardie LA, Timofeeff MN, Demicco RV. 2003. Secular variation in seawater chemistry and the origin of calcium chloride basinal brines. *Geology* 31:857–60

Lyons TW, Berner RA. 1992. Carbon sulfur iron systematics of the uppermost deep-water sediments of the Black Sea. *Chem. Geol.* 99:1–27

Lyons TW, Luepke JJ, Schreiber ME, Zieg GA. 2000. Sulfur geochemical constraints on Mesoproterozoic restricted marine deposition: lower belt supergroup, northwestern United States. *Geochim. Cosmochim. Acta* 64:427–37

Lyons TW, Severmann S. 2006. A critical look at iron paleoredox proxies: new insights from modern euxinic marine basins. *Geochim. Cosmochim. Acta* 70:5698–722

Melezhik VA, Fallick AE, Rychanchik DV, Kuznetsov AB. 2005. Palaeoproterozoic evaporites in Fennoscandia: implications for seawater sulphate, the rise of atmospheric oxygen and local amplification of the delta C-13 excursion. *Terra Nova* 17:141–48

Miller KG. 2005. The Phanerozoic record of global sea-level change. *Science* 310:1293–98

Millero FJ. 1991. The oxidation of H_2S in Framvaren Fjord. *Limnol. Oceanogr.* 36:1006–14
Mort HP, Adatte T, Follmi KB, Keller G, Steinmann P, et al. 2007. Phosphorus and the roles of productivity and nutrient recycling during oceanic anoxic event 2. *Geology* 35:483–86
Murphy AE, Sageman BB, Hollander DJ. 2000. Eutrophication by decoupling of the marine biogeochemical cycles of C, N, and P: a mechanism for the Late Devonian mass extinction. *Geology* 28:427–30
Murphy AE, Sageman BB, Hollander DJ. 2001. Eutrophication by decoupling of the marine biogeochemical cycles of C, N, and P: a mechanism for the Late Devonian mass extinction: comment and reply: reply. *Geology* 29:470–71
Murray JW, Stewart K, Kassakian S, Krynytzky M, DiJulio D. 2007. Oxic, suboxic, and anoxic conditions in the Black Sea. In *The Black Sea Flood Question: Changes in Coastline, Climate, and Human Settlement*, ed. V Yanko-Hombach, A Gilbert, N Panin, PM Dolukhanov, pp. 437–52. Dordrecth, Netherlands: Kluwer
Nederbragt AJ, Thurow J, Vonhof H, Brumsack HJ. 2004. Modelling oceanic carbon and phosphorus fluxes: implications for the cause of the late Cenomanian Oceanic Anoxic Event (OAE2). *J. Geol. Soc.* 161:721–28
Newton RJ, Pevitt EL, Wignall PB, Bottrell SH. 2004. Large shifts in the isotopic composition of seawater sulphate across the Permo-Triassic boundary in northern Italy. *Earth Planet. Sci. Lett.* 218:331–45
Newton RJ, Wignall PB, Bottrell SH, Metcalfe I. 2007. Degassing of oceanic H_2S and its delivery to terrestrial ecosystems during the Permo-Triassic extinction. In *Goldschmidt Conference*. Cologne, Ger.: Geochem. Soc.
Nielsen JK, Shen Y. 2004. Evidence for sulfidic deep water during the Late Permian in the East Greenland Basin. *Geology* 32:1037–40
Oguz T. 2002. Role of physical processes controlling oxycline and suboxic layer structures in the Black Sea. *Glob. Biogeochem. Cycles* 16(2):1019
Olcott AN, Sessions AL, Corsetti FA, Kaufman AJ, de Oliviera TF. 2005. Biomarker evidence for photosynthesis during Neoproterozoic glaciation. *Science* 310:471–74
Overmann J, Beatty JT, Hall KJ, Pfennig N, Northcote TG. 1991. Characterization of a dense, purple sulfur bacterial layer in a meromictic salt lake. *Limnol. Oceanogr.* 36:846–59
Overmann J, Cypionka H, Pfennig N. 1992. An extremely low-light-adapted phototrophic sulfur bacterium from the Black Sea. *Limnol. Oceanogr.* 37:150–55
Overmann J, Sandmann G, Hall KJ, Northcote TG. 1993. Fossil carotenoids and paleolimnology of meromictic Mahoney Lake, British Columbia, Canada. *Aquat. Sci.* 55:31–39
Pancost RD, Crawford N, Magness S, Turner A, Jenkyns HC, Maxwell JR. 2004. Further evidence for the development of photic-zone euxinic conditions during Mesozoic oceanic anoxic events. *J. Geol. Soc.* 161:353–64
Poulton SW, Fralick PW, Canfield DE. 2004. The transition to a sulphidic ocean ~1.84 billion years ago. *Nature* 431:173–78
Raiswell R, Berner RA. 1985. Pyrite formation in euxinic and semi-euxinic sediments. *Am. J. Sci.* 285:710–24

Raiswell R, Buckley F, Berner RA, Anderson TF. 1988. Degree of pyritization of iron as a paleoenvironmental indicator of bottom-water oxygenation. *J. Sedimentary Pet.* 58:812–19

Raiswell R, Canfield DE. 1996. Rates of reaction between silicate iron and dissolved sulfide in Peru margin sediments. *Geochim. Cosmochim. Acta* 60:2777–87

Raiswell R, Canfield DE. 1998. Sources of iron for pyrite formation in marine sediments. *Am. J. Sci.* 298:219–45

Riccardi AL, Arthur MA, Kump LR. 2006. Sulfur isotopic evidence for chemocline upward excursions during the end-Permian mass extinction. *Geochim. Cosmochim. Acta* 70:5740–52

Ridgwell A, Hargreaves JC, Edwards NR, Annan JD, Lenton TM, et al. 2007. Marine geochemical data assimilation in an efficient Earth system model of global biogeochemical cycling. *Biogeosciences* 4:87–104

Rimmer SM. 2004. Geochemical paleoredox indicators in Devonian-Mississippian black shales, central Appalachian basin (USA). *Chem. Geol.* 206:373–91

Ripley EM, Shaffer NR, Gilstrap MS. 1990. Distribution and geochemical characteristics of metal enrichment in the New Albany Shale (Devonian-Mississippian), Indiana. *Econ. Geol. Bull. Soc. Econ. Geol.* 85:1790–807

Roychoudhury AN, Kostka JE, Van Cappellen P. 2003. Pyritization: a palaeoenvironmental and redox proxy reevaluated. *Estuar. Coast. Shelf Sci.* 57:1183–93

Ryan WBF, Cita MB. 1977. Ignorance concerning episodes of ocean-wide stagnation. *Mar. Geol.* 232:197–215

Sarmiento JL, Herbert T, Toggweiler JR. 1988. Causes of anoxia in the world ocean. *Glob. Biogeochem. Cycles* 2:115–28

Schlanger SO, Jenkyns HC. 1976. Cretaceous oceanic anoxic events: causes and consequences. *Geol. Mijnb.* 55:179–84

Schouten S, van Kaam-Peters HME, Rijpstra WIC, Schoell M, Damste JSS. 2000. Effects of an oceanic anoxic event on the stable carbon isotopic composition of Early Toarcian carbon. *Am. J. Sci.* 300:1–22

Schultz RB. 2004. Geochemical relationships of Late Paleozoic carbon-rich shales of the Midcontinent, USA: a compendium of results advocating changeable geochemical conditions. *Chem. Geol.* 206:347–72

Sheehan PM. 2001. The Late Ordovician mass extinction. *Annu. Rev. Earth Planet. Sci.* 29:331–64

Shen Y, Knoll AH, Walter MR. 2003. Evidence for low sulphate and anoxia in a mid-Proterozoic marine basin. *Nature* 423:632–35

Models relationship between phosphate and sulfide accumulation in an estuarine basin.

Shen YN, Canfield DE, Knoll AH. 2002. Middle Proterozoic ocean chemistry: evidence from the McArthur Basin, northern Australia. *Am. J. Sci.* 302:81–109

Sigman DM, Haug GH. 2003. Biological pump in the past. In *Treatise on Geochemistry*, ed. H Elderfield, pp. 491–528. Oxford: Elsevier Pergamon

Skei J. 1988. Framvaren—environmental setting. *Mar. Chem.* 23:209–18

Sorensen KB, Canfield DE. 2004. Annual fluctuations in sulfur isotope fractionation in the water column of a euxinic marine basin. *Geochim. Cosmochim. Acta* 68:503–15

Stanley DJ. 1978. Ionian Sea sapropel distribution and late Quaternary paleoceanography in the eastern Mediterranean. *Nature* 274:149–52

Strauss H. 2006. Anoxia through time. In *Past and Present Water Column Anoxia*, ed. LN Neretin, pp. 3–19. Dordrecht, Netherlands: Springer

Thompson JB, Ferris FG, Smith DA. 1990. Geomicrobiology and sedimentology of the mixolimnion and chemocline in Fayetteville Green Lake, New York. *Palaios* 5:52–75

Tonolla M, Peduzzi S, Hahn D, Peduzzi R. 2003. Spatio-temporal distribution of phototrophic sulfur bacteria in the chemocline of meromictic Lake Cadagno (Switzerland). *FEMS Microbiol. Ecol.* 43:89–98

Twitchett RJ, Krystyn L, Baud A, Wheeley JR, Richoz S. 2004. Rapid marine recovery after the end-Permian mass-extinction event in the absence of marine anoxia. *Geology* 32:805–8

Van Cappellen P, Ingall ED. 1996. Redox stabilization of the atmosphere and oceans by phosphorus-limited marine productivity. *Science* 271:293–496

Wang K, Chatterton BDE, Attrep M, Orth CJ. 1993. Late Ordovician mass extinction in the Selwyn Basin, Northwestern Canada—geochemical, sedimentological, and paleontological evidence. *Can. J. Earth Sci.* 30:1870–80

Wang K, Geldsetzer HHJ, Goodfellow WD, Krouse HR. 1996. Carbon and sulfur isotope anomalies across the Frasnian-Famennian extinction boundary, Alberta, Canada. *Geology* 24:187–91

Watanabe K, Naraoka H, Wronkiewicz DJ, Condie KC, Ohmoto H. 1997. Carbon, nitrogen, and sulfur geochemistry of Archean and Proterozoic shales from the Kaapvaal Craton, South Africa. *Geochim. Cosmochim. Acta* 61:3441–59

Weeks SJ, Currie B, Bakun A, Peard KR. 2004. Hydrogen sulphide eruptions in the Atlantic Ocean off southern Africa: implications of a new view based on SeaWiFS satellite imagery. *Deep-Sea Res. Pt. I Oceanogr. Res. Pap.* 51:153–72

Werne JP, Sageman BB, Lyons TW, Hollander DJ. 2002. An integrated assessment of a "type euxinic" deposit: evidence for multiple controls on black shale deposition in the Middle Devonian Oatka Creek Formation. *Am. J. Sci.* 302:110–43

Wignall PB, Hallam A. 1992. Anoxia as a cause of the Permian Triassic mass extinction—facies evidence from northern Italy and the western United States. *Palaeogeogr. Palaeoclim. Palaeoecol.* 93:21–46

Wignall PB, Newton R. 2003. Contrasting deep-water records from the Upper Permian and Lower Triassic of South Tibet and British Columbia: evidence for a diachronous mass extinction. *Palaios* 18:153–67

Wignall PB, Newton R, Brookfield ME. 2005. Pyrite framboid evidence for oxygen-poor deposition during the Permian-Triassic crisis in Kashmir. *Palaeogeogr. Palaeoclim. Palaeoecol.* 216:183–88

Wignall PB, Twitchett RJ. 2002. Extent, duration, and nature of the Permian-Triassic superanoxic event. In *Catastrophic Events and Mass Extinctions: Impacts and Beyond*, ed. C Koeberl, KC MacLeod, pp. 395–413. Boulder, CO: Geol. Soc. Am.

Wilde P, Berry WBN. 1984. Destabilization of the oceanic density structure and its significance to marine extinction events. *Palaeogeogr. Palaeoclim. Palaeoecol.* 48:143–62

Model of C, N, P, and O biogeochemistry demonstrates feedbacks between ocean redox state and P burial.

Wilkin RT, Barnes HL, Brantley SL. 1996. The size distribution of framboidal pyrite in modern sediments: an indicator of redox conditions. *Geochim. Cosmochim. Acta* 60:3897–912

Worthington LV. 1968. Genesis and evolution of water masses. *Meteorol. Monogr.* 8:63–67

Yemenicioglu S, Erdogan S, Tugrul S. 2006. Distribution of dissolved forms of iron and manganese in the Black Sea. *Deep-Sea Res. Pt. I Topical Stud. Oceanogr.* 53:1842–55

Yilmaz A, Tugrul S, Polat C, Ediger D, Coban Y, Morkoc E. 1998. On the production, elemental composition (C, N, P) and distribution of photosynthetic organic matter in the Southern Black Sea. *Hydrobiologia* 363:141–56

Annual Review
of Earth and
Planetary Sciences
Volume 36, 2008

Contents

Indexes

Errata

An online log of corrections to *Annual Review of Earth and Planetary Sciences* articles may be found at http://earth.annualreviews.org